International Telecommunication Union

ITU-R

Radiocommunication Sector of ITU

Report ITU-R M.2220-1

(11/2021)

Calculation method to determine aggregate interference parameters of pulsed RF systems operating in and near the bands 1 164-1 215 MHz and 1 215-1 300 MHz that may impact radionavigation-satellite service airborne and ground-based receivers operating in those frequency bands

M Series

Mobile, radiodetermination, amateur and related satellite services

International Telecommunication Union

Foreword

The role of the Radiocommunication Sector is to ensure the rational, equitable, efficient and economical use of the radio-frequency spectrum by all radiocommunication services, including satellite services, and carry out studies without limit of frequency range on the basis of which Recommendations are adopted.

The regulatory and policy functions of the Radiocommunication Sector are performed by World and Regional Radiocommunication Conferences and Radiocommunication Assemblies supported by Study Groups.

Policy on Intellectual Property Right (IPR)

ITU-R policy on IPR is described in the Common Patent Policy for ITU-T/ITU-R/ISO/IEC referenced in Resolution ITU-R 1. Forms to be used for the submission of patent statements and licensing declarations by patent holders are available from http://www.itu.int/ITU-R/go/patents/en where the Guidelines for Implementation of the Common Patent Policy for ITU-T/ITU-R/ISO/IEC and the ITU-R patent information database can also be found.

Series of ITU-R Reports

(Also available online at http://www.itu.int/publ/R-REP/en)

Series	Title
BO	Satellite delivery
BR	Recording for production, archival and play-out; film for television
BS	Broadcasting service (sound)
BT	Broadcasting service (television)
F	Fixed service
M	**Mobile, radiodetermination, amateur and related satellite services**
P	Radiowave propagation
RA	Radio astronomy
RS	Remote sensing systems
S	Fixed-satellite service
SA	Space applications and meteorology
SF	Frequency sharing and coordination between fixed-satellite and fixed service systems
SM	Spectrum management

***Note**: This ITU-R Report was approved in English by the Study Group under the procedure detailed in Resolution ITU-R 1.*

Electronic Publication
Geneva, 2021

REPORT ITU-R M.2220-1

Calculation method to determine aggregate interference parameters of pulsed RF systems operating in and near the bands 1 164-1 215 MHz and 1 215-1 300 MHz that may impact radionavigation-satellite service airborne and ground-based receivers operating in those frequency bands

(Questions ITU-R 217-2/4 and ITU-R 288/4)

(2011-2021)

TABLE OF CONTENTS

1 Report overview and background

This Report contains a method to calculate the aggregate RF interference (RFI) parameters of in-band and near-band pulsed RFI sources that may impact radionavigation-satellite service (RNSS) airborne and ground-based receivers. The pair of aggregate pulsed RFI parameters calculated by the method can then be used in the general pulsed RFI impact evaluation method for RNSS receivers contained in Recommendation ITU-R M.2030. Detailed examples of the calculation are given in this Report for the cases of RNSS receivers operating in the 1 164-1 215 MHz and 1 215-1 300 MHz bands. Possible application of the method in this Report to higher frequency RNSS bands could be the subject of further study within the ITU-R[1].

1.1 Background for RNSS receivers operating in the 1 164-1 215 MHz band

RNSS receivers in the 1 164-1 215 MHz band may experience pulsed RFI from the composite of in-band and near-band pulsed RF emissions from both ground-based transmitters and airborne transmitters operating in the 960-1 215 MHz band. RNSS receivers, operating near 1 215 MHz, may experience additional pulsed RFI from ground-based radars operating near and above 1 215 MHz. The pulsed emissions composite includes ground-based distance measurement equipment (DME)/tactical air navigation (TACAN) beacon transponders and air traffic control (ATC) secondary surveillance radars (SSRs) together with airborne communication terminals, civilian DME and Traffic Alert and Collision Avoidance System (TCAS) interrogators, and ATC transponders on other aircraft. Airborne RNSS receivers will also encounter continuous RFI from inter- and intra-RNSS satellite signals as well as near-band pulsed and continuous emissions from on-board DME and ATC transmitters. Ground-based RNSS receivers may encounter different levels of RFI from several types of the pulsed and continuous RFI sources.

DME and TACAN are pulse-ranging navigation systems that operate on pairs of 1 MHz channel increments within the 960-1 215 MHz frequency band. DME systems provide relative slant range measurements for aircraft. TACAN, a navigation system operating on the same basic channel plan, provides both relative azimuth and slant range information. The highest carrier frequency for on-board DME/TACAN interrogator transmitters (1 150 MHz) is only 26.45 MHz below the lowest RNSS signals (e.g. L5/E5a) on carrier frequency 1 176.45 MHz. Parts of the world with the densest DME/TACAN concentrations include an area in Europe and three areas in the United States of America.

Some administrations authorize a system that utilizes spread spectrum techniques for terrestrial communication, navigation and identification (CNI) to operate within the 960-1 215 MHz band. This is generally true in the areas of the densest DME/TACAN concentrations mentioned above. This CNI system, which is utilized on surface and airborne platforms within a network, is a frequency-hopping system that operates on 51 different carrier frequencies (3 MHz increments) between 969 MHz and 1 206 MHz.

Widely used ATC and airborne TCAS surveillance systems operating at 1 030 MHz and 1 090 MHz also need to be analysed. These include the ATC Radar Beacon System (ATCRBS) and Mode S secondary surveillance air and ground components, airborne TCAS, and the Mode S Extended-Squitter systems for automatic dependent surveillance. Ground-based radars operating above 1 215 MHz may have an RFI impact to RNSS receivers operating below 1 215 MHz depending on frequency separation and RNSS receiver filter selectivity. These radars are described in § 1.2.

---

[1] While some of the receivers operating in 1 559-1 610 MHz are similar to the receivers operating in the 1 164-1 215 MHz and 1 215-1 300 MHz bands, the sources of interference are different and modeling these sources in the 1 559-1 610 MHz requires further analysis.

Continuous wideband RFI from several source types including intra- and inter-RNSS system satellite signal cross-correlation is also a factor. Intra-RNSS system interference is defined as interference to the acquisition, tracking, and data demodulation due to its own signals. Inter-system interference is defined as interference to the acquisition, tracking, and data demodulation due to other RNSS generated signals and RNSS augmentations. Other continuous RFI sources include unwanted emissions from licensed and un-licensed transmitters and incidental emissions from non-transmitting devices.

1.2 Background for RNSS receivers operating in the 1 215-1 300 MHz band

RNSS receivers in the 1 215-1 300 MHz band may experience pulsed RFI from the composite of in- and near-band pulsed RF emissions from ground-based radars operating in the 1 215-1 390 MHz band, the RFI from amateur radio systems (1 240-1 300 MHz), and continuous wideband RFI from a variety of other sources.

There are many radars operating in and near this band worldwide for a wide variety of surveillance purposes. These radars transmit very high-power pulsed-signals with varied frequencies and varied pulse durations from a few microseconds to a millisecond. These high-power pulsed signals can be in-band or near-band pulsed RFI to the RNSS receivers operating in this frequency band.

The amateur radio service operates at power levels up to 1.5 kW (with many restrictions), using a wide variety of emission types in or near the operating frequency range of RNSS receivers in the 1 215-1 300 MHz band. The unwanted and necessary emissions from these transmitters could potentially cause continuous interference. Pulsed transmission is not allowed.

Spaceborne active microwave sensors under the allocation of the Earth exploration satellite service, (EESS (active)), are also operating in the band 1 215-1 300 MHz. The types of active sensors requiring use of this band include the synthetic aperture radar (SAR) and scatterometer. The characteristics of these active sensors vary, and the details for SAR sensors are contained in a preliminary draft new Report that is under development within the ITU-R. Characteristics of scatterometer sensors have not been addressed yet. Since the pulsed interference from spaceborne EESS (active) systems into an RNSS receiver will usually be dominated by one system, it is important that this methodology and its results be included in the evaluation of pulsed interference into RNSS receivers in the 1 215-1 300 MHz band. Similar to the 1 164-1 215 MHz band, continuous wideband RFI from a variety of sources, including intra- and inter-RNSS system satellite signal cross-correlation, is also a factor.

1.3 Report content

The following sections provide a general methodology for computing aggregate pulsed RFI parameters for emissions of DME/TACAN and other pulsed RF systems on 1 164-1 215 MHz (L5/E5 signals) band RNSS systems, 1 164-1 188 MHz (L5/E5a signals) band RFI environment modelling, and L5 GPS airborne receiver performance analysis results for the US and Europe RFI hot-spots. Initially the focus of the Report was on airborne RNSS receivers. However, RFI effect equations for other more general purpose terrestrial RNSS receivers are also discussed in the Report. The Report also provides the pulsed RFI scenarios and aggregate RFI parameter computation examples for ground-based RNSS receivers in the 1 164-1 215 and 1 215-1 300 MHz bands.

2 Simulation modelling and computation methodology

2.1 Basic computation method

The RFI parameter computation method described in this Report is used to support the classic "source-path-receiver" analysis framework. That framework involves generating or collecting information concerning three basic but interrelated elements: (1) emissions and location information of potential RFI sources; (2) interference path parameters derived from aircraft-RFI source encounter scenarios; and (3) models for receiver performance that include the effects of RFI. In general, the RFI encounter scenario underlies the analysis framework by providing key input elements to all three of its parts. The encounter scenario is based on a specific RNSS receiver operation that dictates such elements as applicable receiver performance requirements, RFI sources that might be present, and encounter geometries (i.e. distances between the receiver and RFI sources, and angles of arrival at the aircraft receive antenna). The information for RFI sources includes locations, antenna characteristics, and emission waveform types, power levels, and frequencies (for consideration in the receiver model). The receiver model provides the means for determining the effects of various interference types on receiver performance parameters.

2.1.1 RNSS receiver operational RFI scenario detailed descriptions

2.1.1.1 High-altitude airborne RFI scenario for 1 164-1 188 MHz

The high altitude RFI scenario for the 1 164-1 188 MHz band (L5/E5a signals) for this Report has the following features:

– The airborne RNSS receiver has dropped out of en-route navigation mode due to an event (e.g. an aircraft power bus outage) that forces acquisition of all satellite signals.

– L-Band pulsed RFI sources (960-1 215 MHz) geometrically distributed to the radio line-of-sight (LoS):
  - in-band ground DME/TACAN beacon transponders;
  - near-band airborne DME/TACAN interrogators (on-board and nearby aircraft);
  - out-of-band (OoB) ATC surveillance systems (ground, on-board and nearby aircraft elements);
  - CNI system networks (ground and nearby airborne terminals).

– Continuous wideband RFI from:
  - intra- and inter-RNSS system satellite signal cross-correlation;
  - unwanted and unintentional wide- and narrow-band RFI from ground-based sources.

NOTE – Near-band emissions from ground-based air surveillance radars (1 215 MHz-1 390 MHz) are believed to have an impact on RNSS receivers operating up to 1 215 MHz but no significant impact on L5/E5a RNSS receivers operating below 1 188 MHz.

Since the most significant pulsed RFI effects are known to be relatively localized and occurring mainly above 20 000 feet mean sea level (MSL), the airborne RNSS receiver is assumed to be in normal en-route navigation mode. For the purpose of analysing satellite signal "warm-start" acquisition after the triggering event is over, the RNSS satellite signals are assumed to be at least at their specified minimum values. Warm-start acquisition is a condition in which the RNSS receiver is able to use various recently-stored situational parameters (satellite ephemerides, aircraft motion, and receiver state) to reduce acquisition time.

2.1.1.2 Low-altitude airborne RFI scenario for 1 164-1 188 MHz

RNSS receivers are susceptible to RFI sources that are both external and internal to the aircraft. The low-altitude (less than 2 000 ft) RFI scenario for the 1 164-1 188 MHz band (L5/E5a signals) for this Report includes:

– Terminal RNAV approach airspace operations
– Pulsed RFI sources in 960-1 215 MHz geometrically distributed to the radio LoS:
  • in-band ground DME/TACAN beacon transponders;
  • near-band airborne DME/TACAN interrogators (on-board and nearby aircraft);
  • OoB ATC surveillance systems (ground, on-board, and nearby aircraft);
  • CNI system networks (ground and nearby airborne terminals).
– Aggregate continuous RFI from the following:
  • intra- and inter-RNSS system satellite signal cross-correlation (wideband);
  • unwanted and unintentional wide- and narrow-band RFI from ground-based sources.

NOTE – Near-band emissions from ground-based air surveillance radars (1 215-1 400 MHz) are believed to have little impact on L5/E5a RNSS receivers operating below 1 188 MHz.

At low altitude, external RFI is a concern from terrestrial CW and continuous broadband emissions. However, on-board RFI from portable electronic devices (PEDs) is assumed not to be a concern because current in-flight rules require PEDs to be turned-off during the aircraft descent, approach, landing, and taxi phases of flight.

RFI from the near-band airborne DME/TACAN interrogators normally increases in the terminal area where a high density of aircraft operates.

In-band ground DME/TACAN beacons transponders, which have significant RFI effects on L5/E5a RNSS receivers at the high-altitude, may have less significant effects on L5/E5a RNSS receivers at the low-altitude.

2.1.1.3 Ground-based RFI scenario for 1 164-1 215 MHz

The RFI scenario for ground-based RNSS receivers in the 1 164-1 215 MHz band applies to:

– RNSS receivers for aircraft surface movement and fixed RNSS reference receivers;
– fixed, portable, and mobile RNSS receivers (other RNSS applications).

The ground-based RFI scenario includes the following sources:

– aggregate continuous RFI from the following:
  • intra- and inter-RNSS system satellite signal cross-correlation (wideband);
  • unwanted and unintentional wide- and narrow-band RFI from ground-based sources;
– pulsed RFI sources in 960-1 215 MHz within the RNSS receive antenna radio LoS:
  • in-band ground DME/TACAN beacon transponders;
  • near-band airborne DME/TACAN interrogators (nearby aircraft);
  • OoB ATC surveillance systems (ground and nearby aircraft);
  • CNI system networks (nearby airborne terminals).

NOTE – Near-band emissions from ground-based air surveillance radars (1 215-1 400 MHz) are believed to have very little impact on RNSS receivers operating below 1 215 MHz.

Ground-based RNSS receivers could see more than one in-band ground DME/TACAN beacon transponders (much less than the number seen by the low- and high-altitude airborne RNSS receivers).

2.1.1.4 Ground-based RFI scenario for 1 215-1 300 MHz

The RFI scenario for ground-based RNSS receivers in the 1 215-1 300 MHz band includes:

– in-band pulsed emissions from ground-based surveillance radars;
– in-band pulsed emissions from spaceborne SAR;
– in-band continuous emissions from the amateur radio transmitters (1 240-1 300 MHz);
– aggregate continuous RFI from the following:
  • intra – and inter-RNSS system satellite signal cross-correlation (wideband);
  • unwanted and unintentional wide- and narrow-band RFI from ground-based sources.

Ground-based surveillance radars transmit very high power pulsed-signals with varied frequencies and varied pulsed durations from a few microseconds to a millisecond. These high-power pulsed signals are in-band/near-band RFI to the RNSS receivers operating in this frequency band. It is believed that ground-based RNSS receivers may experience some RFI impact only from the nearby radars and not so much from the distance radars, due to LoS geometry and blockages.

The amateur radio service operates at power levels up to 1.5 kW (with many restrictions), using a wide variety of emission types. The necessary and unwanted emissions from these transmitters could potentially cause interference. Various narrowband emission types are authorized: CW, modulated CW, and radio-teletype (RTTY), radiotelephone, data, and imagery. In addition, spread spectrum is authorized with transmitter power restricted to 100 W or less. Pulsed transmission is not allowed.

2.2 RNSS receiver models

2.2.1 General RNSS receive system model descriptions

Because of in-band and near-band pulsed RFI, certain RNSS receivers operating in the bands 1 164-1 215 MHz and 1 215-1 300 MHz may use increased frequency selectivity (compared to RNSS receivers in other bands and other RNSS receivers in these bands) and possibly a rapid digital pulse blanking technique. Either blanking or clipping the pulses that saturate the receiver's front-end, can be used. As a rule, compared to blanking, "clipping" the high-level pulses, at the same amplitude level as the blanking threshold, results in twice the loss in dB.

Some RNSS receivers, especially ground-based receivers, might not employ the rapid digital pulse blanking technique. Their RF front-ends can be saturated from high-level pulsed-RFI. However, the RFI pulsed duty cycle (and thus the performance degradation) experienced on the ground is generally less than experienced by the airborne receivers at higher altitudes. Thus normal operation remains feasible. RNSS receivers, operated in these frequency bands, generally experience less pulsed RFI impact if they have a short overload recovery time from saturation. Less stringent RF/IF selectivity may be used outside their passbands compared to that used by airborne receivers.

2.2.1.1 Airborne RNSS receive system model for 1 164-1 188 MHz operation

A set of parameters are developed to address principal performance aspects of an L5 (1 164-1 188 MHz) airborne receiver system. The set defines the receiver system model with which to assess the feasibility of proper performance in the presence of the RFI environment in operational scenarios. Key elements of the assumed model RNSS receiver are a dual-band active antenna and increased-selectivity RF/IF receiver front-end, a digital pulse blanker, and a multiple-correlator signal processor with a sufficient number of correlators for fast searches of the long signal codes (10.230 bits) proposed for the L5/E5 RNSS signals in the 1 164-1 215 MHz band.

To help address OoB and near-band pulsed RFI, airborne RNSS receivers in the 1 164-1 215 MHz band are assumed in this Report to employ a greater selectivity than the existing selectivity of airborne

L1 receivers. The selectivity factor of 5.5 dB/MHz outside the passband of the L5/E5 RNSS airborne receivers is used in this Report.

Because of the large amount of in-band pulsed RFI encountered at high enroute altitudes, airborne RNSS receivers are assumed in this Report to employ a rapid digital pulse blanking mitigation technique. More details are contained in § 2.2.4.1.

2.2.1.2 Descriptions of ground-based RNSS receive system models

Some RNSS receivers, especially those ground-based receivers, may not employ the rapid digital pulse blanking technique. Their RF front-ends can be saturated from high-level pulsed-RFI. However, the saturation pulsed duty cycle experienced on the ground is generally less than experienced by the airborne receivers. The amount of overload recovery time for RNSS receivers, operated in these frequency bands, directly influences the degree of pulsed RFI impact. Some ground-based receivers may employ a rapid digital pulse blanking circuitry with a relaxed RF/IF selectivity, 4 dB/MHz (compared to 5.5 dB/MHz used by airborne receivers) outside their passbands.

Details of several RNSS receiver models and their associated antenna models will be described in subsequent sub-sections. These include airborne and ground-based receiver models in 1 164-1 215 MHz and three ground-based receiver models in 1 215-1 300 MHz.

2.2.2 RNSS receive antenna models

2.2.2.1 Airborne RNSS receive antenna model for 1 164-1 188 MHz

Studies[2] by an aviation standards organization have resulted in a model for lower hemisphere gain of an RNSS antenna installed on an aircraft. The model upper bound gain limit in the lower hemisphere has linear isotropic gain values for the RFI calculations that are –6 dBi at 0°, decrease log-linearly with angle to –10 dBi at –30°, and remain constant at –10 dBi from –30° to –90° elevation.

For aircraft equipped with CAT II/III precision approach, an additional step in the limit to –13 dBi was selected to apply for the elevation angles between –45º and –90º. This choice reflects the need to accommodate the smaller RFI separation distances and associated angles involved. It is also reflects the likelihood that larger body aircraft of the sort equipped for higher performance categories can achieve somewhat lower back-lobe gain.

2.2.2.2 Other RNSS receive antenna models

A precision-performance ground-based antenna, for use with a high-precision RNSS receiver operating in the 1 164-1 215 MHz band, is designed to limit the multipath effects coming from ground reflection and other nearby buildings/obstacles. It also achieves very-low phase error at the same time by utilizing both advanced spiral technology and a self-complementary element structure. The antenna is designed for uniform gain in azimuth. This antenna is right-hand circular polarization (RHCP) and has antenna gains of –9 dBi or better at 5-degree elevation angle and better than –3 dBi at zenith.

Similar performance is required of an SBAS ground reference receive antenna operating in the 1 215-1 300 MHz band. The antenna is RHCP and has antenna gains of –5 dBi maximum at 0° elevation angle, better than –3 dBi at zenith, and uniform gain in azimuth.

---

[2] RTCA SC-159, *Assessment of radio frequency interference relevant to the GNSS L5/E5a frequency band*, Document No. RTCA/DO-292, July. 2004, Appendix, G.3.4.

2.2.3 RNSS receiver RF front-end model parameters

2.2.3.1 Airborne 1 164-1 188 MHz band RNSS receiver RF front-end model parameters

Because of OoB and near-band RFI including that from on-board pulsed transmitters, it is expected that RNSS L5/E5 aeronautical receiver standards may benefit from a higher selectivity than existing L1 receiver standards. The selectivity response (see Fig. 1) assumed within this Report shows a 5.5 dB/MHz skirt attenuation for frequency offset from the passband corner frequency. This attenuation profile is assumed to be achieved through a set of filters distributed throughout the receiver's front-end (including in the antenna pre-filter) and does not include the contribution of the PRN code correlation process. Feasibility of the selectivity was assessed, in part, by signal flow analysis[3] of a cascaded network of realistic receiver components (amplifiers, mixers, RF and IF filters) with amplifier gain compression effects included. In the pulsed RFI analysis the selectivity curve is applied as if it were concentrated at the antenna terminals to appropriately reduce the power level of near-band and OoB pulsed signals prior to comparison with the pulse blanking threshold.

FIGURE 1

Frequency-dependent rejection vs. offset from L5/E5a centre frequency

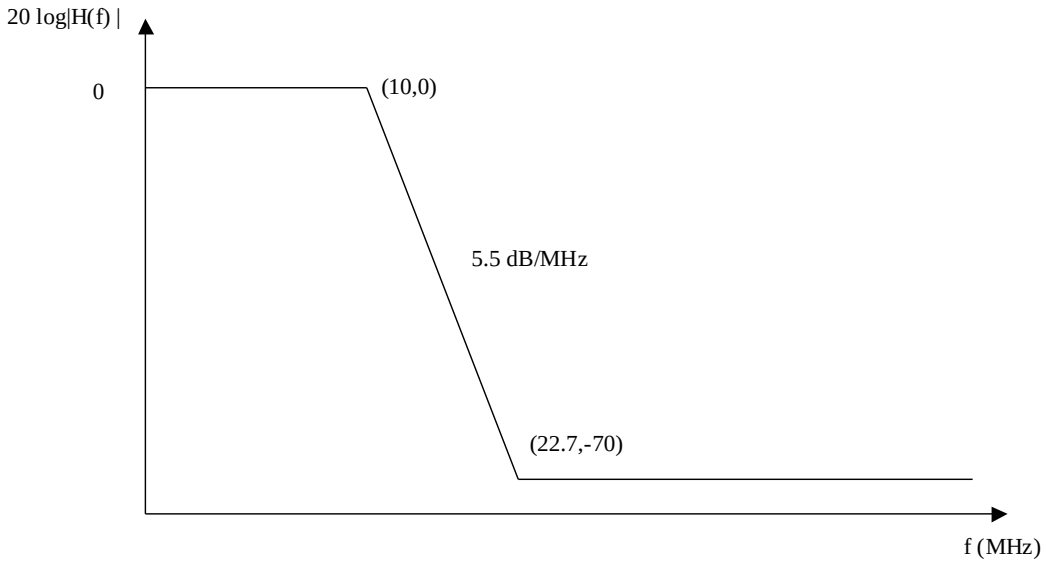

One consequence of the increase in selectivity and peak pulse power handling as compared to L1 receivers is a higher receiver input noise temperature, due primarily to increased pre-filter insertion and limiter losses. The equivalent input thermal noise density is assumed to be –200 dBW/Hz for L5/E5a (as compared to –201.5 dBW/Hz assumed at L1). A typical L5/E5a receiver noise budget to justify the –200 dBW/Hz value is shown in Table 1.

[3] RTCA SC-159, *Assessment of radio frequency interference relevant to the GNSS L5/E5a frequency band*, Document No. RTCA/DO-292, July. 2004, Appendix, D.2.3.

TABLE 1

Typical L5/E5a receiver system noise budget

Parameter	Value	Comment
Preselector filter insertion loss (dB)	2.19	Higher than typical L1 value (due to increased selectivity)
Limiter loss (dB)	0.5	Higher than typical L1 value (due to increased peak pulse power handling req't)
Low noise amplifier (LNA) noise figure (NF) (dB)	1.8	Same as L1; includes impedance mismatch
Receiver – processor noise figure contribution (dB)	0.6	Assumes 13 dB cables losses antenna-to-receiver, ~30 dB LNA gain, 7 dB receiver NF
Receiver input noise figure (dB)	5.0	Sum of above items
Equiv. receiver input temp (K)	627	$(10^{NFdB/10} - 1)$*290 K
Sky temperature (K)	100	Same as L1
System input noise temp (K)	727	$T_{SYS} = T_{SKY} + T_{RCVR}$
System input noise spectral density (dBW/Hz)	−200	$k \cdot T_{SYS}$, 1.5 dB higher than L1 due to higher selectivity, power handling req't.

2.2.3.2 RF front-end model parameters for ground-based RNSS receivers

Both 1 164-1 215 MHz and 1 215-1 300 MHz band SBAS ground reference receivers operate in the pulsed environment and the multipath environment. Consequently, those receivers are assumed to use various means, including rapid digital pulsed RFI suppression technology to address in-band and adjacent band interference from pulsed DME/TACANS, radars, and other pulsed-systems. The receiver filter is designed to have linear phase characteristics over the ±10 MHz bandwidth. The 10 MHz filter will be used to attenuate the OOB emissions with at least 4 dB/MHz roll-off to a −70 dB max attenuation. The receivers are also designed to stay locked on both code and carrier in the presence of a single interferer with −20 dBW peak power, 1 ms pulse width, and a 10% duty cycle. Both receivers employ the narrow correlator tracking technology to minimize the multipath effects and provide the most accurate reference signal measurements at the same time.

2.2.4 RNSS receiver pulsed RFI effects

2.2.4.1 Pulse blanking architecture model

The airborne RNSS L5/E5 receiver is assumed to employ rapid digital pulse blanking, or a technique that achieves equivalent performance in a high pulsed RFI environment. Other blanking methods or a pulse clipping implementation could also be considered, for example, but with significantly less efficiency or more loss. As a rule, "clipping" the high-level pulses, at the same amplitude level as the blanking threshold, results in twice the degradation (dB) to C/N_0. The block diagram below (Fig. 2) shows how digital pulse blanking might be implemented ahead of the signal correlators in an RNSS receiver.

FIGURE 2

Block diagram of a typical digital pulse blanking receiver

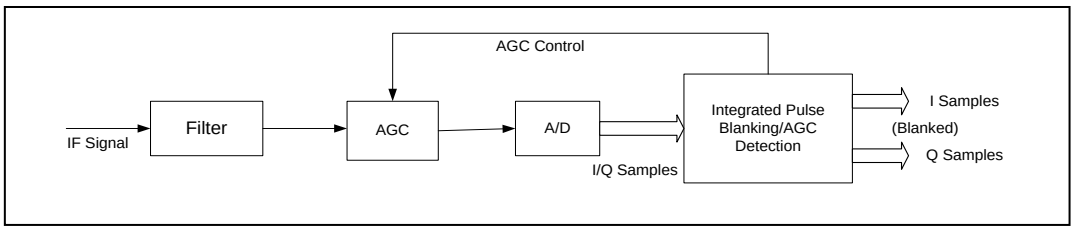

Rapid response in the digital blanking, or an equivalent mechanization, is also important. In general, the digital pulse blanking receiver uses automatic gain control (AGC), which excludes detected pulses from the gain calculations. It is important that the AGC recovery quickly, ideally in less than 5 ms. Careful AGC implementation is necessary to minimize the *A*/*D* quantization losses. Any blanking delay allows part of the strong pulse to enter the correlator (albeit clipped), in addition to continued blanking (and resulting signal loss) after the pulse subsides. The result is a combination of clipping and increased pulse duty cycle.

Pulses that saturate the receiver's front-end will be blanked or clipped, depending upon mechanization. However, depending upon the level of saturation, pulse stretching will occur to some degree, effectively increasing the blanking duty cycle. Thus, it is important that this stretching be kept at a minimum. Fortunately, except for onboard pulsed signals, saturation should not occur in a well-designed receiver/antenna. When it does, the duty cycle of such pulses should be relatively low if careful gain distribution is considered. The effect of the blanking threshold value is further discussed in § 2.3.1.

2.2.4.2 Pulse saturation architecture model

Certain RNSS receivers operating in the RNSS bands, for example, ground-based applications may not be subjected to large amounts of in-band and near-band pulsed RFI as airborne RNSS receivers. As such, they may not contain pulse blanking circuitry as described in § 2.2.4.1 above, but rather will be saturated briefly by RFI pulses from nearby sources. The block diagram of a typical pulse-saturation receiver is similar to the block diagram in Fig. 2 above, without the pulse-blanking circuitry. Pulse saturation architecture model may be employed for ground-based RNSS receivers/ equipment. In-band pulses will typically saturate the last gain stage first. Near band interference will tend to saturate the intermediate gain stages with medium level input interference, and OoB interference signals will saturate only the first RF stage of the front-end. This characteristic is due to the interspersing of filters between each RF and Intermediate Frequency (IF) gain stage, which leads to increasing frequency selectivity as the interference signal proceeds through the front-end. The saturation pulse duty cycle is much less than experienced by the airborne receivers. Still, it is important that pulse-saturation RNSS receivers, operated in this frequency band, have a short recovery time.

2.3 RNSS receiver pulsed RFI effects theory

2.3.1 Pulse blanking effects theory

In this Report the theoretical equation to compute the effective C/N_0 for a pulse blanking receiver has been updated from ones used in earlier studies. In algebraic terms it is:

$$\left(C/N_{0,EFF}\right)=\left(\frac{C}{N_0}\right)\frac{\left(1-PDC_B\right)}{\left(1+\frac{I_{0,WB}}{N_0}+R_I\right)} \quad (1)$$

where:

C: post-correlator (interference-free) RNSS satellite carrier power (W)

N_0: receiver system thermal noise density (W/Hz)

$I_{0,WB}$: total wideband equivalent continuous RFI power spectral density (PSD) (W/Hz) (in case that other RNSS interference is included, spectral separation coefficient (SSC) should be properly taken into account)

PDC_B: (pulse duty cycle-blanker) is the net aggregate duty cycle of all pulses strong enough to activate the blanker (unitless fraction)

R_I: unitless post-correlator ratio of total aggregate below-blanker average pulsed RFI power density to receiver system thermal noise density N_0.

R_I is given by:

$$R_I = \left(\frac{1}{N_0 \cdot BW} \right) \sum_{i=1}^{N} P_i \cdot dc_i \tag{2}$$

where:

N: total number of pulsed emitters that generate received pulses (i.e. pulses or pulse portions) below the blanker threshold

P_i: peak received power (W) of the i-th pulse emitter (referenced to the passive receive antenna output) with peak level below the blanker threshold

BW: pre-correlator IF bandwidth (for spreading effect) (Hz)

dc_i: duty cycle (unitless fraction) of the i-th below-blanker pulsed emitter exclusive of pulse collisions.

The right-hand terms of equation (1) are the following:

– first term – C/N_0 (Hz) in the absence of interference;

– second term (numerator) – Net C/N_0 reduction due to the blanker (1-PDC_b) after accounting for low-level pulse erasures by strong pulse blanking;

– third term (denominator) – Relative increase of the noise floor caused by:

- suppression of receiver system thermal noise, N_0 and total wideband continuous interference, $I_{0,WB}$ densities by the blanker; plus
- noise floor contribution, R_I from low-level pulses adjusted to account for low-level pulse erasures by pulse blanking.

To help streamline the necessary pulsed RFI inpact calculations, an additional term has been defined in relation to equation (1). The term ‘effective noise density ratio’, $N_{0,EFF}$, which combines the pulsed RFI effects on thermal noise density, wideband continuous RFI density, and signal loss, is defined algebraically as:

$$N_{0,EFF} = \frac{N_0}{(1 - PDC_B)} \left(1 + \frac{I_{0,WB}}{N_0} + R_I \right) \tag{3}$$

and in logarithmic form as:

$$N_{0,EFF}(dB) = 10 \cdot \left[\log(N_0) - \log(1 - PDC_B) + \log\left(1 + \frac{I_{0,WB}}{N_0} + R_I \right) \right] \tag{4}$$

The term $N_{0,EFF}$ is quite flexible in handling the varying amounts of continuous and pulsed RFI encountered in both high and low altitude aircraft as well as other operational scenarios. The second and third log terms within the brackets combine to form the updated 'degradation factor' used in earlier US and European studies. In the limit where the effective continuous wideband RFI density, $I_{0,WB} = 0$, $N_{0,EFF}$ reduces to the pulsed RFI degradation effect. In the other limit where both PDC_b and $R_I = 0$, $N_{0,EFF}$ reduces to the conventional form ($N_0 + I_0$).

PDC_b, the composite aggregate strong pulse blanking factor from the operations of multiple heterogeneous pulsed systems, is given as:

$$PDC_b = 1 - \prod_j \left(1 - PDC_{bj}\right) \tag{5}$$

where the symbol $\prod_j$ denotes multiplication carried over the system index, j, with, for example, $PDC_{b1} = PDC_{b,TACAN/DME}$, $PDC_{b2} = PDC_{b,CNI}$, etc. This formulation assumes that strong pulse blanking effects from heterogeneous systems are stochastically independent.

Also, R_I (the algebraic form in equation (2)), the aggregate weak pulse RFI contribution (i.e. pulses or pulse portions below blanker threshold) is compiled as the simple sum over the system index, j, of the R_i factors determined separately for each pulsed system. That is:

$$R_I = \sum_j R_{i,j} \tag{6}$$

Note, by the way, the R_I term appears in relation to the continuous RFI terms in equation (1), that the net pulsed noise contribution has been adjusted to account for strong pulse blanking erasures even though R_I and its component parts are computed without assuming erasures. The adjustment was made algebraically at the composite level by dividing out the common factor (1-PDC_B) from each denominator term to cancel an equal numerator factor.

The version of equation (1) used in earlier studies conservatively assumed that neither strong nor low-level/weak pulses collide with each other[4,5]. More recent software and hardware validation efforts[6], however, revealed that this conservatism is too severe especially for high altitude analysis of the TACAN/DME RFI in high concentration regions. In those instances the gross strong pulse duty cycle without considering pulse collisions can approach or even exceed 100%. The critical findings incorporated in equations (1), and (4)-(6) that reduce this conservatism are as follows:

– accounting for strong pulse overlays (power above the pulse blanking threshold);
– erasure of weak pulses (below the blanking threshold) by strong pulse blanking;
– residual portion of Gaussian DME/TACAN pulse after the pulse blanking;
– pulse blanking and erasure interaction among heterogeneous pulses from the DME/TACAN, CNI systems, and ATC systems.

More details of the pulse overlap model derivation are in Annex B.

---

4 ITU-R Document 8D/113.

5 Hegarty, C., *et al*., "Methodology for determining compatibility of GPS L5 with existing systems and preliminary results," *Proceedings of The Institute of Navigation Annual Meeting*, Cambridge, MA, June 1999.

6 Op. cit., RTCA/DO-292, Appendix E, § E.5, E.6.

One implicit pulse blanking parameter known to have a significant effect on results is the blanking threshold value. Early analyses used a blanking threshold power value of −86.5 dBm in a 20 MHz pre-correlator bandwidth. More recent work[7] has led to the choice of a −90 dBm in a 20 MHz pre-correlator bandwidth value which appears close to optimum for a range of relative contributions from weak and strong pulsed RFI sources. For all analyses to date the threshold defines a fixed, abrupt boundary between blanked intervals and un-blanked pulsed noise intervals. A fixed threshold may not be practical to use in an actual GPS receiver design; receiver gain and noise variations would likely suggest use of an adaptive threshold. However, differences due to assuming an ideal fixed threshold in predicted blanking performance compared to actual measured performance appear to be insignificant[8].

2.3.2 Pulse RFI effect equation for a saturating RNSS receiver

Certain RNSS receivers operating in the 1 164-1 215 MHz or 1 215-1 300 MHz band in ground-based applications may not subjected to large amounts of in-band and adjacent band pulsed RF interference as air-navigation receivers are. As such, they may not contain pulse blanking circuitry as described in § 2.3.1 but rather will be saturated briefly by RFI pulses from near-by sources. The presence of pulsed RFI reduces the amount of continuous RFI that the RNSS receiver can tolerate.

The effects of both pulsed and continuous RFI for a saturating RNSS receiver can be quantified, similar to equation (3), by defining an effective post-correlator noise power spectral density, $N_{0,EFF}$, as:

$$N_{0,EFF} = \frac{N_0\left[\left(1+\frac{I_{0,WB}}{N_0}+R_I\right)\left(1+\frac{N_{LIM}{}^2 PDC_{LIM}}{\left(1-PDC_{LIM}\right)}\right)\right]}{\left(1-PDC_{LIM}\right)} \tag{7a}$$

where, similar to equation (2):

$$R_I = \left(\frac{1}{N_0 \cdot BW}\right)\sum_{i=1}^{N} P_i \cdot dc_i \tag{7b}$$

In the above equations,

N_0 : receive system thermal noise PSD (W/Hz) (= kT_{SYS})

$I_{0,WB}$: total wideband equivalent continuous RFI PSD (W/Hz)

PDC_{LIM} : aggregate fractional duty cycle of the saturating RFI pulses (unitless)

R_I : ratio of aggregate below-saturation average pulse RFI power density to N_0 (unitless ratio)

N_{LIM} : ratio of receiver A/D saturation level to 1σ noise voltage established by AGC (unit-less ratio)

P_i : peak received RFI power of the *i*-th below-saturation level pulsed emitter (W), (referenced to the receiver passive antenna terminal)

BW : pre-correlator IF bandwidth (for spreading effect) (Hz) and

dc_i : duty cycle (unitless) of the *i*-th low-level RFI signal exclusive of pulse collisions.

All the noise and interference terms in equations (7a) and (7b) are referenced to the receive system passive receive antenna terminals. The parameter N_{LIM} is a receiver parameter that is determined by

---

7 Op. cit., RTCA/DO-292, Appendix D.3.

8 *Ibid*, Appx. E.6.

the analogue-to-digital conversion implementation. For the simplest hard-limiting RNSS receiver (with a "1-bit" quantizer), N_{LIM} = unity. Since, in that case, the receiver limits on noise, the RFI parameter R_I is essentially zero. In more general cases, R_I is related to the receiver saturation level and the peak power and pulse duty cycle of below-saturation RFI pulses. Note that when no the pulsed RFI is present, the RFI parameters, PDC_{LIM} and R_I are zero and equation (7a) reduces to $N_{0,EFF} = N_0 + I_{0,WB}$, a familiar definition for continuous RFI analysis. Note also that if N_{LIM} is set to zero, equation (7a) reduces to the identical form as equation (3) for a pulse blanking receiver.

Given a maximum value for $N_{0,EFF}$ and the set of pulsed RFI parameters, equation (7a) can be solved for the allowable aggregate continuous wideband PSD for the non-RNSS interference component.

Equations identical in form to equations (5) and (6), respectively, are used to compute aggregate values for PDC_{LIM} and R_I from a composite of several pulsed sources. For scenarios with large values of PDC_{LIM}, the pulsed RFI degradation for the saturating receiver tends to be larger than for a pulse blanking receiver.

2.3.3 Total aggregate wideband continuous interference effect

When analysing the effect of pulsed RFI to RNSS receivers it is necessary to quantify the total amount of continuous RFI that is also present. The combined effect of continuous and pulsed RFI must remain below some specific limit to permit proper RNSS receiver operation. In general, since that combined RFI effect limit is fixed for a given receiver type or application, the amount of pulsed RFI that can be tolerated depends on the amount of continuous RFI present and vice versa. As noted in the definitions above, the term, $I_{0,WB}$, is used to represent the total wideband equivalent continuous RFI PSD present at the RNSS receive antenna. To minimize the complexity of the pulsed RFI analysis, the $I_{0,WB}$ term is assumed to be a fixed value representing the baseline condition.

The total PSD $I_{0,WB}$, represents the sum of several component terms that include, in general, both non-RNSS and RNSS continuous RFI. As such, it is generally larger in value than the continuous RFI threshold values for the various receivers contained in several RNSS receiver characteristics Recommendations. That difference is due at least in part to the explicit exclusion of RNSS RFI[9] from those threshold values. Some specific safety applications may also have excluded certain other components from the listed non-RNSS RFI thresholds, but these excluded components must be added into the total for $I_{0,WB}$.

2.3.4 Usage limits for effective noise power spectral density, $N_{0,EFF}$, equations

For RFI pulse width values from 0.1 to 1 000 ms, the $N_{0,EFF}$ defining equations described in §§ 2.3.1 and 2.3.2 above have been shown to be properly represent the pulsed RFI effect on RNSS receivers operating in signal tracking mode in the 1 164-1 215 MHz and 1 215-1 300 MHz bands. For some RNSS receivers operating in the signal acquisition mode, the equations also properly represent the pulsed RFI effect over the same RFI pulse width range as long as associated pulse duty cycles remain moderate.

For certain RNSS receiver operating in the acquisition mode with small accumulation time (about 1 to 2 ms), further study may be needed to determine the usage limits for high duty cycle and long interference pulse width and verify the equation predictions.

---

9 See Recommendation ITU-R M.1831 for a discussion of methodology to determine the RNSS intra- and inter-system RFI.

3 Pulsed RF source emission models and airborne receiver aggregate pulse parameters

3.1 Pulsed RF source emission models for airborne RNSS receivers

3.1.1 DME/TACAN system pulsed emission models

3.1.1.1 DME/TACAN system overview

The DME navigation system consists of airborne interrogators and ground-based beacon transponders. The TACAN system has airborne interrogators and both ground and airborne transponders. DME ground transponder beacons operate in one of four modes (X, Y, W, Z) (Fig. 3). TACAN beacons use only the X and Y modes. Ground beacons operating in the X-mode (the dominant civil mode) radiate within the band segments 962-1 024 MHz (channels 1X–63X) and 1 151-1 213 MHz (channels 64X–126X). A majority of en-route/high altitude sites radiate on frequencies in the upper band. Only those X mode beacons in the 1 151-1 213 MHz band segment are sufficiently close in frequency to impact operation of proposed future RNSS systems.

FIGURE 3

DME/TACAN mode and channel frequency plan

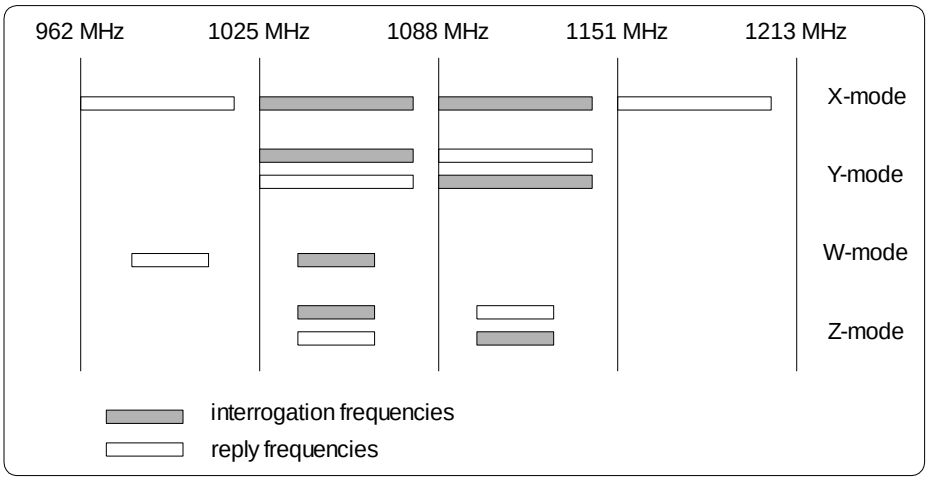

An aircraft interrogator transmits a randomized, low-rate sequence of pulse pairs with the specific mode-dependent intra-pair spacing on one of 126 frequencies from 1 025 to 1 150 MHz (1 MHz increments). For each correctly-spaced interrogation pulse pair received, the X-mode ground beacon transmits, after a fixed time delay, a reply pulse pair with an intra-pair spacing of 12 μs. The beacon also transmits randomly-timed pulse pairs triggered by the beacon receiver noise (commonly called squitter). The overall beacon transmission rate is held constant by varying beacon receiver sensitivity such that, when there are insufficient interrogations, the squitter transmissions triggered by receiver noise are increased. In the USA, ground DME transponders radiate an average of 2 700 pulse pairs per second (ppps) inclusive of ID Tone. TACAN transponders also insert coded azimuth reference pulses, for an average of 3 600 ppps. The average pulse pair rate assumptions of 2 700 ppps for DME and 3 600 ppps for TACAN are well accepted as a worst-case scenario and are used for the simulations in this Report.

3.1.1.2 DME/TACAN ground beacon model

At high altitudes in a few regions around the world (e.g. US airspace surrounding Harrisburg, PA, Chicago, IL, and Fresno, CA), a large number of DME/TACAN beacons are within radio LoS of an airborne RNSS receiver. Figure 4 shows the DME and TACAN sites with frequency assignments from 1 157-1 209 MHz surrounding Harrisburg, Pennsylvania. The outer and inner circles show the geometric LoS limits seen from 40 000 feet and 20 000 feet above MSL respectively. For the Harrisburg case there are about 40 beacons within LoS at 40 000 feet with received power above −100 dBm.

Ground beacons transmit with a peak e.i.r.p. ranging from 100 to 15 000 W. Most (~90%) of the radiated power is contained within a 0.5 MHz bandwidth centred on the 1 MHz channels. The majority of the DME beacons in Fig. 4 have 4 kW e.i.r.p. while most of the TACAN beacons have 13.8 kW. These values assume a 6 dBi peak antenna gain (net of cable/installation losses) for both beacon types. Relative antenna elevation gain patterns for operational TACAN and DME antennas used in the analysis are shown in Fig. 5.

FIGURE 4

DME/TACAN beacons around Harrisburg, PA
(channels 70X to 122X, Radio LoS circles for 20 kft and 40 kft MSL)

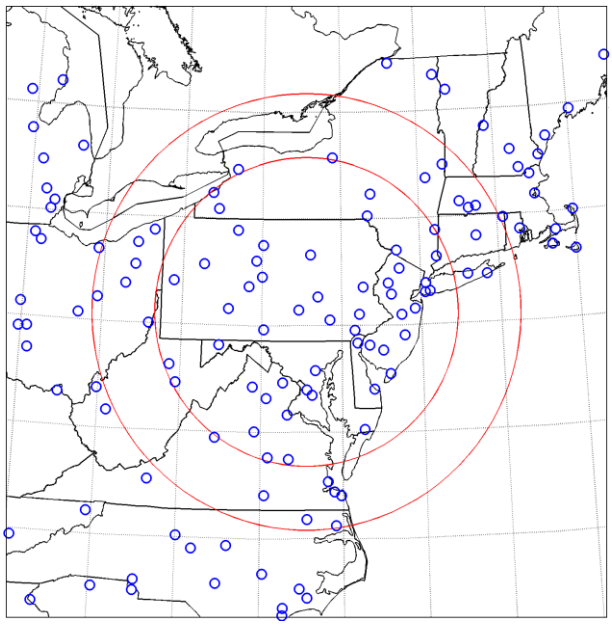

FIGURE 5

Typical DME/TACAN antenna normalized gain vs. elevation angle (962 MHz, 0° az) (peak gain – cable losses = 6 dBi – Data source: *dB-Systems*)

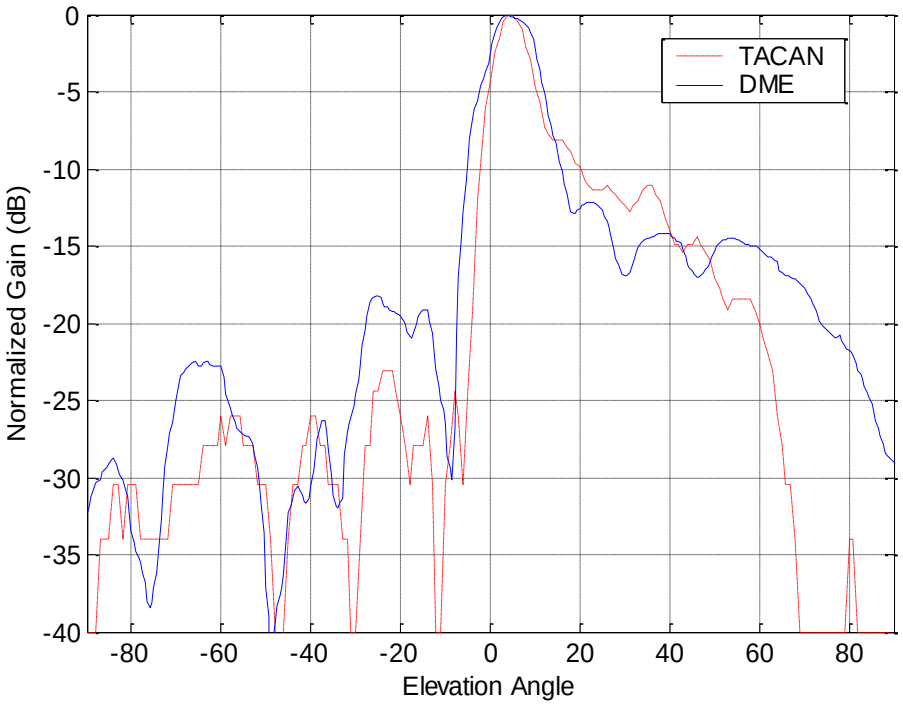

3.1.1.3 Rectangular equivalent pulse width

Because DME and TACAN beacons transmit Gaussian envelope pulses, the meaning of pulse width must be defined before computing RFI duty cycle for pulses above the blanking threshold (PDC_B in equation (1)), and below the blanking threshold (dc_i in equation (3)). Ideal DME/TACAN Gaussian pulses having 3.5 μs pulse width (50% peak voltage level) are described analytically[10] by an instantaneous power envelope as:

$$p(t) = P_{pk} \exp(-\alpha t^2) \tag{8}$$

with $\alpha = 4.51*10^{11} s^{-2}$ (t = 0 is pulse mid-point).

For low-level pulses, where P_{pk} is below the blanker threshold, the rectangular equivalent PW_{eq} is defined as:

$$PW_{eq} = \frac{1}{P_{pk}} \int_{-\infty}^{\infty} p(t)dt \tag{9}$$

Substituting equation (8) with the given value of α into equation (9) and performing the integration yields PW_{eq} = 2.64 μs.

The above-blanker width of strong pulses is defined by the time period that the instantaneous received power envelope exceeds the blanker threshold. Given the received DME/TACAN peak power, P_{REC}, and the pulse blanking threshold power, P_{THR}, the blanking pulse width x, can be obtained by defining the above-threshold power ratio as $\frac{P_{THR}}{P_{REC}} = e^{-\alpha t^2}$.

[10] Op. cit., Hegarty, "Methodology Results," *Proc. of the ION Annual Meeting,* Cambridge, MA, June 1999.

Solving for t and substituting $x = 2t$ yields the above-blanker pulse width:

$$x = 2t = 2\sqrt{\frac{\ln\left(P_{REC} / P_{THR}\right)}{\alpha}} \tag{10}$$

The below-threshold portions of strong Gaussian pulses have an equivalent pulse width in terms of the complementary error function (*erfc*) as:

$$PW_{eq} = erfc\left(\sqrt{\alpha} \cdot w\right) \tag{11}$$

where $w = x/2$.

These pulse widths are then multiplied by the appropriate pulse repetition rate (2 700 ppps, DME or 3 600 ppps, TACAN) to obtain the desired duty cycle value. The weak pulse and below-threshold strong pulse duty cycle values are used to find the average power of these two contributions to the effective pulse/noise ratio.

The above-blanker (equation (10)) and residual below-blanker (equation (11)) equivalent pulse widths for strong DME/TACAN pulses are plotted (Fig. 6) as functions of peak received pulse power for a blanker threshold of −90 dBm in the precorrelator bandwidth[11]. Note that pulses with peak power up to about 6 dB above the blanker threshold contribute measurably both to the individual source pulse blanker duty cycle, PDC_b, and to the average below-blanker noise power ratio R_i. When pulses exceed the threshold more than 6 dB, the effect is to PDC_b.

FIGURE 6

Blanker pulse width and residual equivalent pulse width vs. peak power (Pulse blanker threshold = −90 dBm)

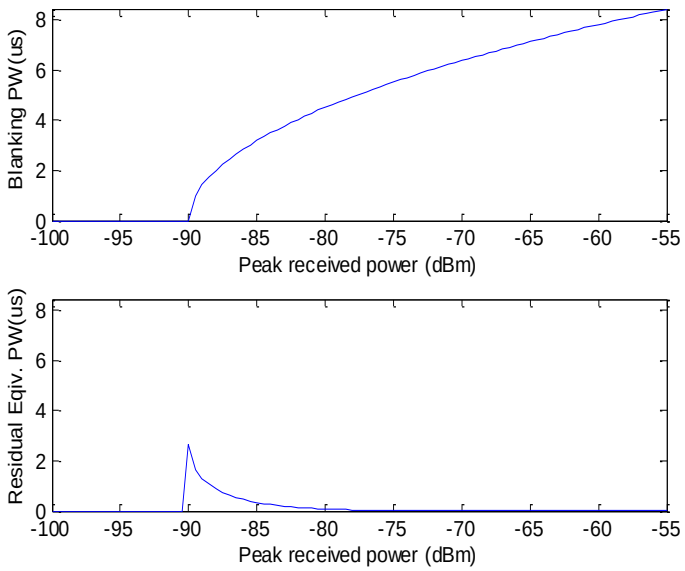

[11] The precorrelator bandwidths are specified in an RNSS receiver characteristics Recommendation for the band 1 164-1 215 MHz in development within the ITU-R.

3.1.2 CNI system pulsed emission model

3.1.2.1 CNI system overview

The CNI system authorized to operate in some administrations is a spread-spectrum, frequency-hopping system that currently operates on 51 carrier frequencies at 3 MHz increments distributed between 969 MHz and 1 206 MHz (Fig. 7). Transmitters are limited to radiate 200 W so there is potential for interference in situations where a CNI system equipped aircraft is flying in the close vicinity of aircraft equipped with GPS L5 or there is a large amount of CNI system activity in the area.

FIGURE 7

CNI system channel frequencies

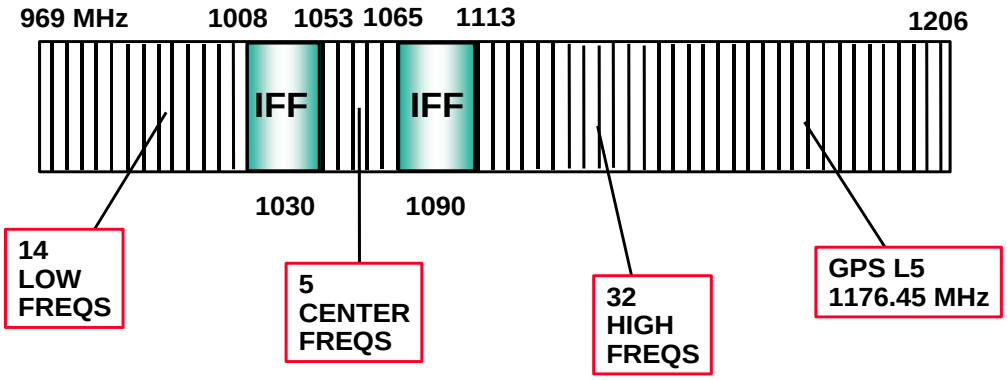

A time division multiple access (TDMA) approach is used to accommodate multiple user terminals within a given network. The TDMA time structure contains 128 timeslots/s (7.8125 ms slot duration). Network operations are organized around 12 second frames (1 536 timeslots per frame). A timeslot (Fig. 8) contains either 72[12], 258, or 444 pulses depending on the message structure. The time duration in the slot after the message burst is used for propagation delay. Each pulse in the slot is 6.4-μs long (measured at the 90% power point) and consists of 32 contiguous, 200-nanosecond duration, phase-modulated chips (continuous phase shift modulation). The 6.4 μs pulse is followed by 6.6 μs off time for a 13.0 μs basic pulse period. The carrier frequency is switched during the off-time.

[12] 72 pulses for one terminal, but 144 pulses are possible for multiple terminal transmissions during a round trip timing message.

FIGURE 8

CNI system timeslot and pulse transmission structure

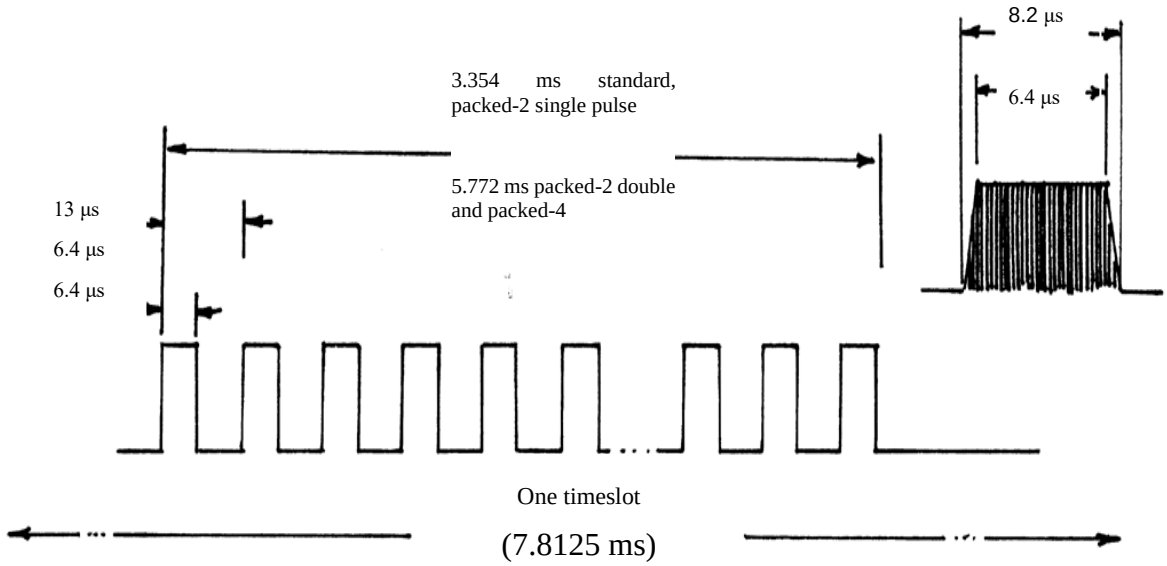

3.1.2.2 CNI system operational model

The authorization in the various administrations for the CNI system in the 960-1 215 MHz band is predicated on controlling the time slot duty factor (TSDF) within a defined geographical area (GA). TSDF is a measure of the total number of CNI system pulses transmitted by a single platform, a single network or within a geographic area. A 100% TSDF (single network maximum capacity) equates to the total number of pulses resulting from a 258 pulse transmission occurring in every one of the 1 536 time slots over 12 seconds. Thus, 100% TSDF is defined as an environment of 396 288 pulses in 12 seconds, distributed evenly among the 51 CNI system carrier frequencies. While other administrations manage CNI system transmitted TSDF at various levels within their sovereign territories, within the US airspace, the TSDF is managed to be no more than 100% within a 185 km (100 nmi) radius of any CNI system terminal (see Fig. 9). Within a 370 km (200 nmi) radius the TSDF is managed to be no more than 400% (i.e. three networks maximum within the annulus from 185 km to 370 km radius). In addition, the TSDF from an individual user is managed to be no greater than a 50% TSDF, i.e. no more than 198 144 pulses in a 12 second frame.

Two cases have been shown to bound the RFI effects from the CNI system network scenarios (labeled Case 1 and Case 8 for correspondence to the defining study). These cases are denoted by their TSDF designators as 100/50/(0)/(0) and 100/50/(300)/(300) respectively. Referring for Case 1 to the geographic area (Fig. 9), the 100/50 denotes the “local” net with a single 50% TSDF user in the foreground (i.e. closely separated from the victim receiver) and the remaining 50% TSDF distributed among the rest of the participants in this net all within a 100 nmi radius of the RNSS victim receiver.

FIGURE 9

CNI system geographic area pulse densities

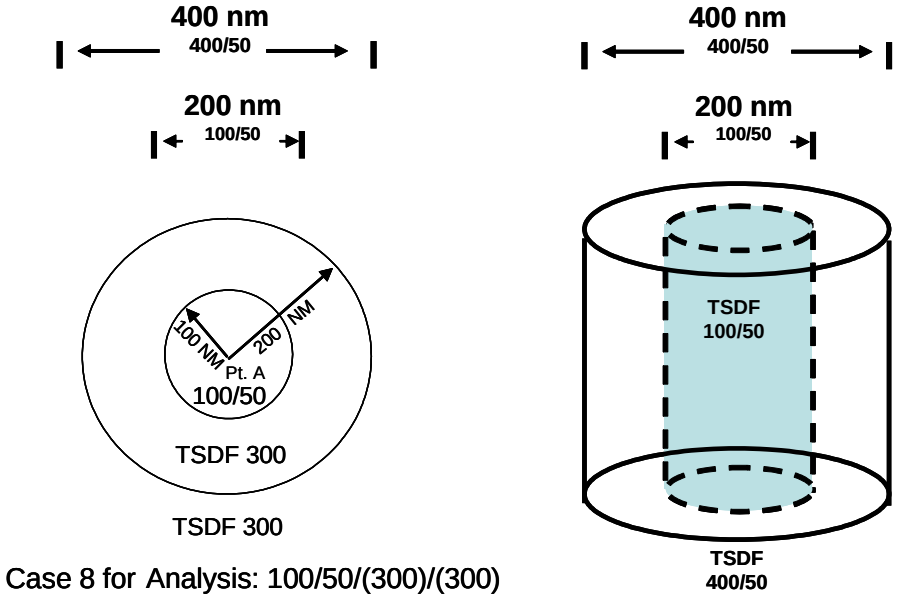

In Case 8 there are also three fully loaded nets within the annulus between 100 and 200 nm from the victim (300% TSDF) and an additional three nets distributed outside the 200 nm radius. Each of the component TSDFs are assigned a fixed received power at the victim RNSS antenna port, chosen to reflect worst case EMC operational conditions for test purposes. The RNSS receiver is chosen to be in close proximity to the 50% TSDF emitter. For this analysis there are 4 categories of users based on received power. The received power from the 50% foreground user is set at −34.5 dBm; the remaining 50% of local users (Ring 1) are all received at –60 dBm. In addition, for Case 8 the received power is −90 dBm from all users between 100 and 200 nm (Ring 2) and the users in the 3 remote nets beyond 200 nm are all received at −100 dBm (Ring 3).

3.1.2.3 CNI system pulse emission analysis

The CNI system emission analysis assumes (without loss of generality) that each user is transmitting standard 258 pulse messages (Fig. 8), with a message burst occupying 3.354 ms in a 7.8125 ms time slot (i.e. 258 pulses with an inter-pulse interval of 13 μs, each pulse of nominal 6.4 μs width at peak power of 200 W). Because of the pulse-by-pulse frequency hopping, two expressions are needed to determine the average pulse duty cycle (cast in terms of a 100% TSDF user category): They are:

$$dc_{ab}(x, N_c) = \frac{8.4 \cdot 258 \cdot x}{7812.5 \cdot N_c} \tag{12a}$$

and:

$$dc_{bb}(N_c) = \frac{7.2 \cdot 258}{7812.5 \cdot N_c} \tag{12b}$$

Equation (12a) (for $dc_{ab}(x, N_C)$) is used to calculate the duty cycle for pulses received above the blanker threshold. The aggregate dc_{ab} value for all CNI system terminals in each particular case is $PDC_{B,CNI}$. For above-blanker pulses, the nominal 6.4 μs pulse width is increased to 8.4 μs to account for the shaped CPSM pulse base and 'pulse stretching' in the RNSS receiver blanking circuitry. The parameter, x, is the number of pulses above the blanker threshold and N_C is the number of pseudo-randomly selected carriers (either 51 or 37).

Similarly, equation (12b) (for $dc_{bb}(Nc)$) is used to calculate the duty cycle of pulses received below blanker threshold. The 7.2 μs pulse width is the nominal value at 50% amplitude. The dc_{bb} values for the different user categories are used in the calculation of $R_{I,CNI}$ as described in a subsequent paragraph.

Note that since the received power is fixed for each of the (4) CNI system user categories, what happens in a single timeslot accrues for every time slot allocated to that category of user. For example, if 15 of the 51 carriers from the 50% TSDF foreground user are above threshold, its duty cycle contribution to PDC_B is 0.5 $dc_{ab}(15,51)$ = 0.039.

The received power of each of the frequency-hopped carriers has to be "conditioned" by the frequency dependent rejection (FDR) of a 20 MHz GPS/WAAS band pass filter (shown in Fig. 1). A CNI system pulse spectrum mask (Fig. 10) has been defined to reflect the actual CPSM spectrum. The mask indicates −10 dBc emission at ±3 MHz away from centre frequency, then has a constant roll-off down to −60 dBc at ±15 MHz to reflect an average 'noise floor' in any 3 MHz band beyond ±15 MHz from the carrier.

FIGURE 10

CNI system pulse spectral mask

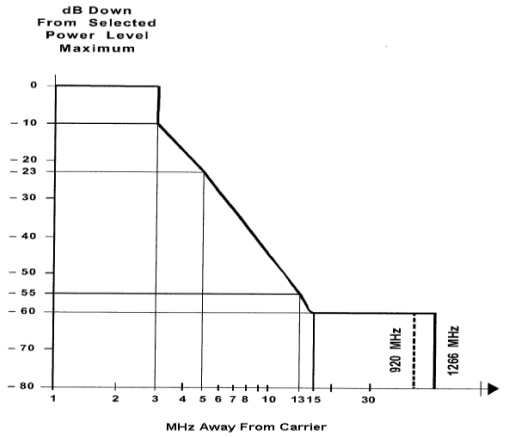

The FDR for each of the 51 carriers is calculated using this mask (relative to 0 dBc) and the resulting in-band powers then adjusted by the peak received power assigned to each user category. It is then a simple matter to determine how many carriers are above blanker threshold to calculate dc_{ab} for each user category as well as the actual in-band power for each carrier/pulse received below threshold to be then multiplied by dc_{bb} as a contribution to R_i.

The collected results of this process are summarized in Table 2 for both the Case 1 and Case 8 scenarios which lists the PDC_b and R_i factors for 51 carrier usage as well as 37 remapped carriers for a blanker threshold of –90 dBm.

TABLE 2

CNI system pulsed RFI parameters

CNI system scenario	51 carriers		37 carriers	
	PDC_b	R_I	PDC_b	R_I
Case 1	0.073	0.059	0.101	0.049
Case 8	0.073	0.296	0.101	0.377

Case 1 results are more appropriate for use in some landing and take-off operational scenarios and are included here for comparison. Case 8 results are used for mid-and high-altitude airborne RNSS operational scenarios analysed in this Report.

3.1.3 ATC ground and airborne surveillance pulsed emission models

The systems analysed in this section include the ATCRBS and Mode S secondary surveillance systems (both airborne transponders and ground radar components), TCAS airborne surveillance interrogators, and the Mode S Extended Squitter (for Automatic Dependent Surveillance-B (ADS-B)) systems in a projected environment for 2020. The transmission rate from ATCRBS Mode A, Mode C, and Mode S transponders depends on the number and characteristics of ground radars and airborne (TCAS) interrogators. The TCAS interrogator transmission rate in turn depends on the number of nearby aircraft. Thus, the interference generated by these airborne sources is dependent on the environment in which they are operating.

For many years, the Los Angeles Basin in the United States of America has been considered to be the worst case in terms of peak airborne traffic count with a forecast of up to 750 aircraft within 130 km (70 nmi) of Los Angeles International Airport (LAX) in 2020. Given this density of airborne emitters, the major source of interference comes from transponder replies to ATCRBS and Mode S interrogations which, in turn, is driven primarily by the interrogator density. The LA-area ground interrogator density is also high; there are currently 24 ground interrogators within 120 km (65 nmi) of LAX and 52 within 200 nm of LAX, all of which can interrogate aircraft close to LAX. An additional 46 emitters between 370 and 925 km (200-500 nmi) can interrogate aircraft above FL200 in the LAX area. This density is similar to that seen along the US East Coast.

3.1.3.1 ATC surveillance systems modelling approach

The general approach for these systems is to define distributions, uniform in area, for each of the ground emitter and aircraft emitter populations which are based on the LA Basin densities given above. These distributions form an extended background (BG) RFI environment which will primarily contribute to the "below blanker" R_{Ii} effects. In particular, a worst-case ground interrogator density (24 in 120 km radius) equates to emitters in a uniform (equilateral) triangular grid separated from each other by about 46 km (25 nmi). Similarly, 750 aircraft within a 130 km radius are configured in uniform triangular grid of airborne emitters separated from each other by about 9.3 km (5 nmi). To further simplify the analysis, each BG emitter in a same-system distribution is assumed to have the same effective radiated power (ERP) and transmit duty factor.

In addition to the BG distribution, a foreground (FG) emitter is located near to the victim RNSS receiver to determine worst case effects of combined 'above blanker', PDC_b and net 'below blanker', R_i contributions. Also, where appropriate, on-board ATC transmitter effects are included that potentially contribute to the overall PDC_b and R_i factors. Further details on the modelling approach are contained in an RTCA document[13].

3.1.3.2 ATC surveillance systems pulsed RFI parameter results

The results are presented in the Table 3 below for two cases: a generic case and a specific high altitude case. The generic case uses a combination of worst-case assumptions without regard to any particular aeronautical operational scenario or actual operational limitations based on the classic Los Angeles basin environment model. For the high altitude case used for the analyses in this Report, the generic case parameters are adjusted to reflect appropriate high altitude operational constraints.

---

[13] Op. cit. RTCA/DO-292, Appendix E, § E.1, E.2.

TABLE 3

ATC/surveillance systems RFI parameters

Analysis case	PDC_b	R_I
Generic	0.0017	0.0610
High altitude	0.0014	0.0414
Approach/Landing	0.0093	0.0031

Generic case: This case (from an earlier US government interagency study) reflects a trade-off analysis to obtain a worst-case effect. A RNSS receiver-equipped aircraft with on-board Mode S/TCAS/ADS-B equipment is located above a Mode-S ground sensor producing pulses at a level just below the pulse blanker threshold (slant range about 2 290 feet for sidelobe transmissions). That Mode-S ground sensor is interrogating 700 Mode S airborne transponders. The airborne FG emitter is an ATCRBS transponder-equipped aircraft replying to main-beam interrogations from 50 secondary surveillance radars (SSRs) while located about 885 m (2 900 ft.) above the victim aircraft (again with pulse power just below the dBm blanker threshold of −90 dBm in the pre-correlator bandwidth). The airborne emitter (BG) distribution is evenly divided into ATCRBS and Mode S equipped aircraft. Each group is uniformly distributed with 10.5 km (5.66 nmi) separation and shifted so that the combined distribution is equivalent to a uniform-in-area triangular grid with 7.4 km (4 nmi) separation between emitters. Each ATCRBS transponder in the BG is replying to interrogations from 200 SSRs on average (i.e. at 900 replies/s = 75% of the average reply-rate limit) and each Mode-S transponder is on the roll call list of four ground Mode-S interrogators. The RNSS receiver-equipped aircraft is also participating in TCAS and ADS-B transactions.

High altitude case: The Mode S/TCAS/ADS-B/RNSS-equipped aircraft is at 40 000 ft and therefore at least 12 km (6.5 nmi) from the nearest Mode-S ground interrogator. The airborne BG emitter assumptions are altered by placing 90% of the airborne emitters below the 40 000 feet altitude of the RNSS-equipped aircraft (RNSS receive antenna gain, G_{Rb} = −7 dBil), and 10% above the victim (with G_{Ra} = +4 dBil). Each ATCRBS transponder is transmitting at the reply rate limit (1 200 replies/s). The FG transponder, 700 m (2 300 feet) above the RNSS aircraft, is also at the 1 200 replies/s limit.

3.1.4 Airborne ARNS (DME/TACAN) interrogator pulsed emission models

The on-board DME interrogator transmitter outputs 500 W peak RF pulses in the 1 025-1 150 MHz band. The large pulsed power at relatively close physical spacing and small frequency separation (26.45 MHz minimum to the L5/E5a carrier, 1 176.45 MHz) provide the motivation for modelling pulsed RFI effect. The effect was modelled by first computing the peak power level coupled to the RNSS antenna from the DME antenna. From a survey of typical coupling factors for different aircraft types, the DME-to-RNSS antenna coupling loss was set at 45 dB (typical small body aircraft, bottom-mount blade-to-top-mount patch antenna). The interrogator transmitter power at the bottom-mounted blade antenna was assumed to be 24 dBW (27 dBW transmitter output – 3 dB line loss). Thus, the peak DME transmit power at RNSS antenna terminals is −21 dBW, a value large enough to cause concern about RNSS receiver front-end saturation.

Next a candidate antenna preselector circuit having performance consistent with the receiver front-end noise figure and selectivity constraints was modelled and characterized by a detailed steady-state and transient analysis[14]. The analyses show an antenna unit preselector frequency-dependent rejection of 27 dB is achievable at 1 150 MHz for a 4-resonator miniature RNSS bandpass centred at 1 176.45 MHz. The resultant peak power at the RNSS antenna unit LNA input is −48 dBW

[14] Op. cit., RTCA/DO-292, Appendix E.2.

(= −21 dBW −27 dB) or 2 dB above the LNA input compression point. The transient analysis shows that, for the DME pulsed signals between 1 130 and 1 150 MHz, the DME driven pulse waveshape is preserved through the preselector filter with no appreciable transient features added.

Since the interrogator signal is offset at least 26.45 MHz from the L5/E5a centre frequency, accumulated RF and IF filtering in the RNSS receiver will substantially attenuate the DME signal before it reaches the receiver digitizer. However, active stages up through the receiver first mixer and IF amplifier could undergo gain suppression. As an approximation to the actual off-frequency saturation RFI effect, the interrogator pulse width is assumed to be stretched by saturation from the nominal 3.5 μs out to 8.5 μs (high power pulse limit in Fig. 6). Thus, the interrogator pulse pair will have a total on-time of 17 μs.

The on-board DME installation is assumed to have 2 channelling interrogators. Each one has a track-mode interrogation rate of 3 × 20 ppps (3 beacons tracked) 85% of the time and 150 ppps (acquisition mode) 15% for an average rate of 75 ppps. Therefore, the single interrogator duty cycle (pulse pair rate × on-time) = $75*17*10^{-6} = 0.001275$ and the dual DME installation total on-board pulse duty cycle, PDC_b is 0.0026. Below-blanker average power/noise ratio, R_I is assumed to be zero (all on-board RFI impact included in the effective duty cycle).

For interrogators on nearby aircraft a similar arrangement of aircraft is assumed as in the ATC surveillance systems analysis. The nearest aircraft slant range is 700 m (2 300 ft) and its interrogator e.i.r.p. is 27 dBW, The combined effect of R^{-2} loss, average upper hemisphere RNSS antenna gain, and full RNSS receiver FDR yields RFI pulses at –130.8 dBW peak (10.8 dB below blanker threshold). A single DME duty cycle (dc_i, no pulse stretching) = $75*7*10^{-6} = 5.25*10^{-4}$ thus R_i (= P_i dc_i/N_0 BW) is –36 dB. Combining with an estimated upper bound 9 dB aggregation factor for the contribution of all nearby aircraft gives total R_I = 0.002. Thus, the overall airborne DME interrogator pulse RFI components are: $PDC_{B,\ ARNS\ Onboard}$ = 0.0026, and R_I = 0.002.

3.2 Aggregate pulse parameters for airborne RNSS receivers in the 1 164-1 188 MHz band

3.2.1 DME/TACAN beacon aggregate pulse parameters – high altitude airborne RNSS case

The DME/TACAN beacon component RFI parameters (PDC_B and R_I) were computed at FL400 (40 000 ft) using the GREET modelling tool (details in Annex A). GREET calculated these terms along with the $N_{0,EFF}$ degradation at locations on a 0.5° × 0.5° grid spacing using the degradation terms in equation (4) (§ 2.3). Table 4 shows the points of strongest DME/TACAN beacon RFI in the Eastern PA region in the USA (centred on 40N × 76W). The list of DME/TACANs that collectively contributes to the worst RFI at 40N × 76W is included in Attachment A, Table 15. Figure 11 shows $N_{0,EFF}$ degradation contours at FL400 over CONUS for DME/TACAN beacon RFI only.

TABLE 4

DME/TACAN beacon aggregate RFI parameters

(40.5°N × 76.5°W) PDC_b = 0.6284 R_I = 0.4672* **$\Delta N_{0,EFF}$ = 5.96 dB**	(40.5°N × 76.0°W) PDC_b = 0.6103 R_I = 0.4162 **$\Delta N_{0,EFF}$ = 5.60 dB**	(40.5°N × 75.5°W) PDC_b = 0.6049 R_I = 0.4493 **$\Delta N_{0,EFF}$ = 5.64 dB**
(40.0°N × 76.5°W) PDC_b = 0.6084 R_I = 0.4849 **$\Delta N_{0,EFF}$ = 5.79 dB**	(40.0°N × 76.0°W) PDC_b = 0.6121 R_I = 0.5424 **$\Delta N_{0,EFF}$ = 5.99 dB**	(40.0°N × 75.5°W) PDC_b = 0.6002 R_I = 0.4129 **$\Delta N_{0,EFF}$ = 5.48 dB**

TABLE 4 (*end*)

(39.5°N × 76.5°W) PDC_b = 0.6042 R_I = 0.4699 **$\Delta N_{0,EFF}$ = 5.70 dB**	(39.5°N × 76.0°W) PDC_b = 0.5958 R_I = 0.4649 **$\Delta N_{0,EFF}$ = 5.59 dB**	(39.5°N × 75.5°W) PDC_b = 0.5978 R_I = 0.4321 **$\Delta N_{0,EFF}$ = 5.52 dB**

NOTE – The $\Delta N_{0,EFF}$ factors are calculated for only DME/TACAN pulsed RFI using the ratio term in equation (4) ($I_{0,WB}$ = 0). The centre cell (40 N × 76 W) is the 'Harrisburg hot-spot'.

FIGURE 11

US DME/TACAN beacon $N_{0,EFF}$ degradation factor contours at FL400

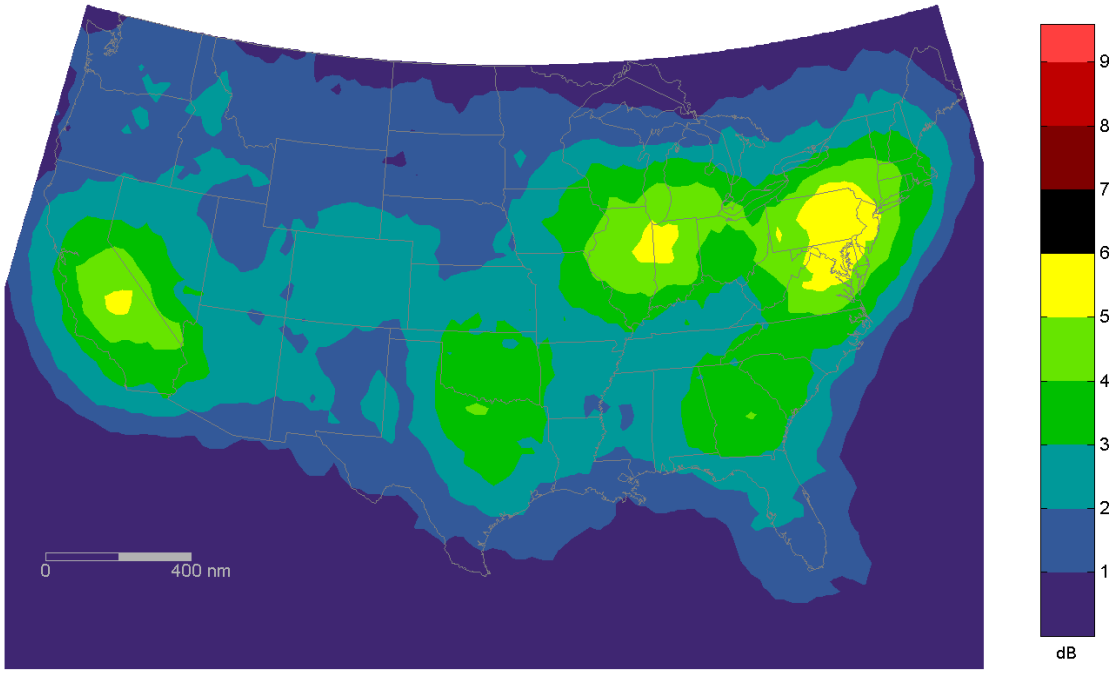

3.2.2 Composite aggregate pulse parameters – high altitude airborne RNSS case

The composite pulsed RFI component parameters for the various systems as described in § 3.1 and applicable to the US hot-spot are summarized in Table 5. The DME/TACAN beacon RFI components are for the 40° N × 76° W "Harrisburg hot-spot" location (Table 4), the CNI system parameters are for Case 8/37 carriers (Table 2), and the ATC system RFI parameters are for the high altitude case (Table 3). Figure 12 shows the overall $N_{0,EFF}$ degradation contours at FL400 over the continental USA.

TABLE 5

High altitude US hot-spot pulsed RFI composite parameters

RFI source	$PDC_{B,j}$	$R_{I,j}$
DME/TACAN ground beacons	0.612 1	0.542 4
CNI system networks (case 8/37 carrier)	0.101 0	0.377 0
ATC/surveillance. sys (ground, airborne)	0.001 4	0.041 4
DME interrogators (onboard, nearby a/c)	0.002 6	0.002 0
US RFI scenario composite totals	0.652 7	0.962 8

The same computation method applied to the worst-case European high altitude RFI hot-spot (50.5° N × 9° E at FL400) with its associated concentration of DME beacons yields the composite pulse RFI parameters in Table 6. Here the CNI system parameters are for Case 8 with the standard 51 carrier configuration (Table 2), the assumed configuration in European airspace. ATC/surveillance system and DME interrogator components are assumed to be the same as in US airspace. Figure 13 shows the overall L5/E5a $N_{0,EFF}$ degradation contours at FL400 over Europe.

TABLE 6

High altitude EU hot-spot pulsed RFI composite parameters

RFI source	$PDC_{B,j}$	$R_{I,j}$
DME/TACAN ground beacons	0.570 1	1.182 4
CNI system networks (case 8/51 carrier)	0.073 0	0.296 0
ATC/surveillance. sys (ground, airborne)	0.001 4	0.041 4
DME interrogators (onboard, nearby a/c)	0.002 6	0.002 0
EU RFI scenario composite totals	0.603 1	1.521 8

FIGURE 12

US overall $N_{0,EFF}$ degradation factor contours at FL400

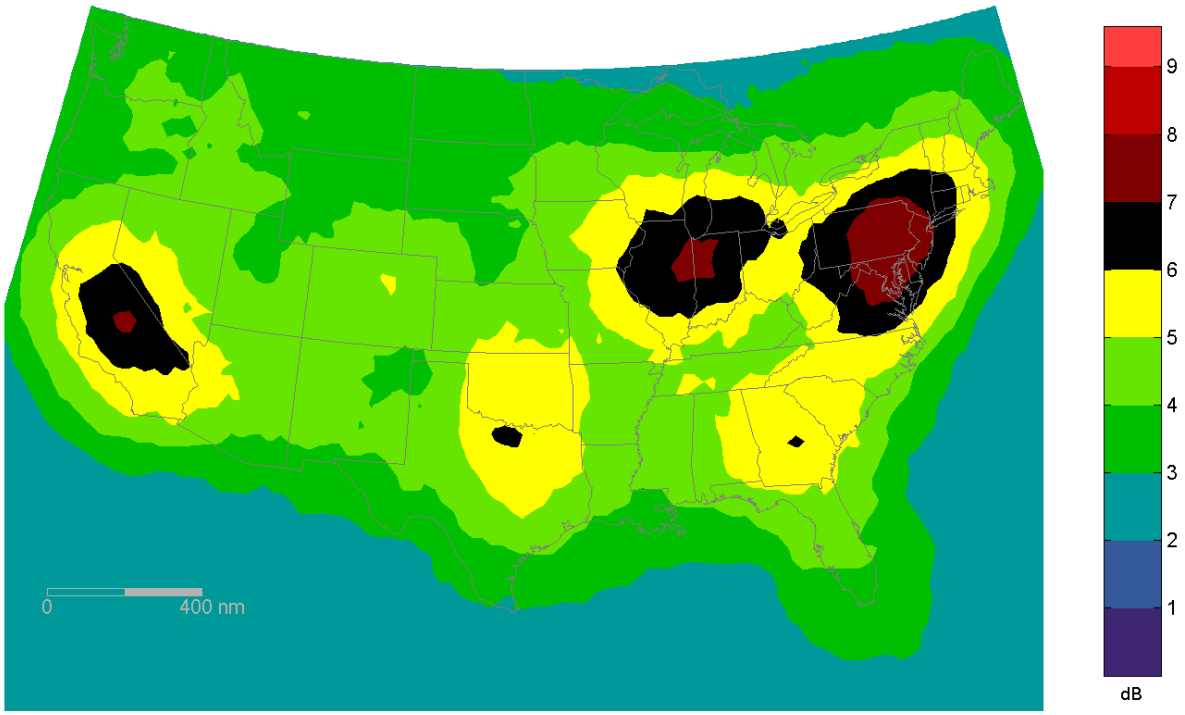

FIGURE 13

Overall L5/E5a $N_{0,EFF}$ degradation contours at FL400 for Europe
(DME/TACAN Beacons, ATC/surveillance, ARNS, CNI System Case 8/51 carrier)

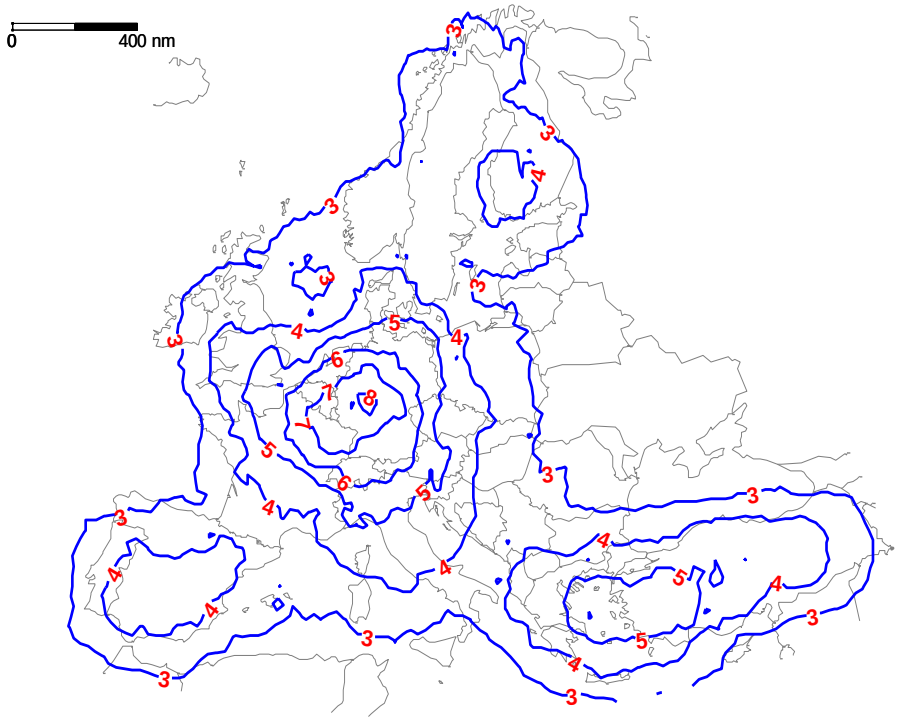

3.2.3 Low-altitude airborne RNSS receiver operational example (1 164-1 188 MHz)

As an illustration at lower altitude of the reduction in pulsed RFI effects principally from DME/TACAN beacons, a representative example is computed for a VOR-DME RNAV/GPS approach to Runway 4 at DCA (Washington Reagan National) airport in the USA. Whether or not this is the worst case, it does show the effect of multiple TACAN beacons visible at the final approach fix waypoint (Teple FAF).

A search of in-band DME and TACAN beacons near existing RNAV routes revealed that Washington/ Reagan National Airport (DCA) is surrounded by multiple TACAN ground beacons within radio LoS (RLoS) at 1 600 ft (Fig. 14).

FIGURE 14

In-band TACANs within RLoS Near DCA

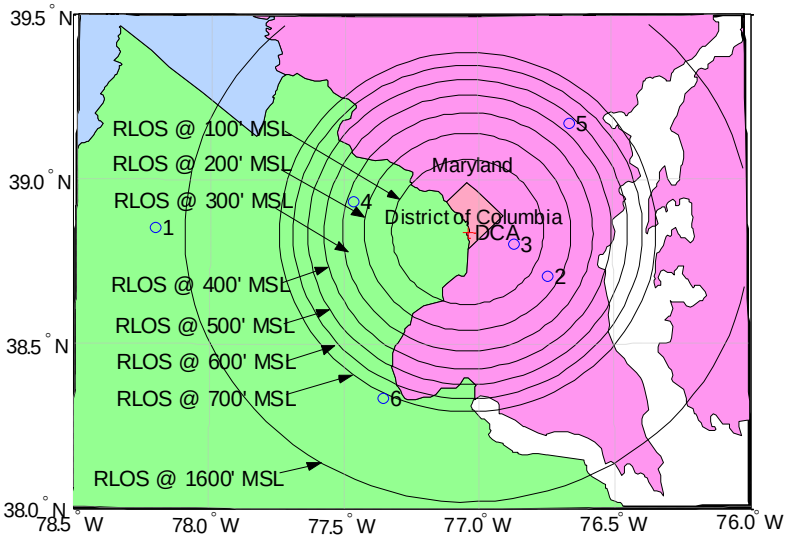

For the stations in view at the Teple final approach fix waypoint, a new set of DME/TACAN beacon pulsed RFI parameters was computed with the GREET tool. The JTIDS and airborne ARNS pulse RFI source component parameters were assumed to be the same as in the high altitude analyses (Table 5). The approach/landing case values (Table 3) were used for the ATC pulsed RFI component.

Teple FAF waypoint component values and the resultant composite parameters are listed in Table 7. The composite total PDC_b and R_I were computed from the component values with equations (5) and (6), respectively. Note the Teple FAF composite values are less than half the Harrisburg composite values in Table 5.

TABLE 7

Low altitude pulsed RFI parameters at Teple FAF

RFI Source	$PDC_{B,j}$	$R_{I,j}$
DME/TACAN ground beacons	0.225 9	0.070 3
CNI system networks (case 8/37 carrier)	0.101 0	0.377 0
ATC/surveillance system (appr/landing)	0.009 3	0.003 1
DME interrogators (onboard, nearby a/c)	0.002 6	0.002 0
US RFI composite totals	0.312 3	0.452 4

4 Aggregate pulsed RFI parameters for ground-based RNSS receivers

4.1 SBAS ground reference receiver pulsed RFI parameters

4.1.1 SBAS ground reference receiver and pulsed RFI source characteristics

The SBAS ground reference receiver operates in the 1 215-1 300 MHz band with an RNSS signal carrier frequency signal at 1 227.6 MHz. As a dual-frequency receiver, it operates simultaneously in the 1 559-1 610 MHz band (RNSS signal carrier frequency at 1 575.42 MHz). The receiver is assumed to have no special pulsed RFI mitigation but instead simply saturates on strong pulses. Other pertinent characteristics are listed in Table 8.

TABLE 8

SBAS ground reference receiver pulse response characteristics[15]

Characteristic	Value
Maximum receive antenna gain – lower hemisphere (dBi)	−5.0 (1)
RF filter 3 dB bandwidth (MHz)	24
Receiver input saturation level (dBW)	−135
Receiver survival level (dBW)	−10
Receiver overload recovery time (s)	1×10^{-6}

(1) This value applies for 5-degree elevation above the horizon.

The pulsed RF sources for this example are assumed to be two surveillance radar transmitter systems operating in the 1 215-1 390 MHz band and located on the ground within the radio horizon of the SBAS ground reference receiver. The separation distances are such that the received peak RFI pulse levels are above the receiver saturation level but below the survival level. The centre frequency for the radar pulses is assumed to lie within or relatively near the receiver RF 3 dB bandwidth (i.e. 1 215.6 to 1 239.6 MHz). Other pertinent characteristics are listed in Table 9.

TABLE 9

Surveillance radar characteristics[16]

Characteristic	Radar A value	Radar B value
Main beam e.i.r.p. (dBW)	101	85.6
Sidelobe e.i.r.p. (dBW)	61	50.6
Transmit pulse width (sec)	2×10^{-6} per pulse	$51.2 \times 10^{-6} \times 2$ pulses
Transmit pulse repetition frequency (Hz)	358	750 per pair

For both radars the beam scanning is such that the SBAS receiver is mostly illuminated by the radar beam side lobes (at ~40 dB below the main beam). At a nominal spacing (several tens of km) from the SBAS receiver, free-space propagation calculations show the sidelobe received peak level is

15 These RNSS receiver characteristic values are taken from Recommendation ITU-R M.1902 for the 1 215-1 300 MHz band, Annex 1, Table 1, Column 1.

16 Parameters for Radars A and B are from Recommendation ITU-R M.1463 for Systems 1 and 5, respectively.

between 56 and 64 dB above the receiver compression level and the main beam peak level is more than 16 dB below the receiver survival level.

4.1.2 SBAS ground reference receiver pulsed RFI parameter calculation

For each saturating pulse RFI source, *i*, in this example, the individual RFI source pulse duty cycle parameter, $PDC_{LIM,i}$, from § 2.3.2 of this Report is computed simply as follows:

$$PDC_{LIM,i} = (PW_i + \tau_R) \cdot PRF_i \quad (13)$$

where:

PW_i : effective received radar pulse width

τ_R : receiver overload recovery time

PRF_i : radar pulse repetition frequency.

For radar A the $PDC_{LIM,i}$ calculation above becomes:

$$PDC_{LIM,A} = (PW_A + \tau_R) \cdot PRF_A = (2+1) \cdot 358 \cdot 10^{-6} = 1.074 \times 10^{-3} \text{ and}$$

for radar B the calculation becomes:

$$PDC_{LIM,B} = (PW_B + \tau_R) \cdot PRF_B = (51.2+1) \cdot 2 \cdot 750 \cdot 10^{-6} = 7.83 \times 10^{-2}.$$

The aggregate PDC_{LIM} is computed with a form of equation (5) from § 2.3.1 of this Report as:

$$PDC_{LIM} = 1 - \prod_j \left(1 - PDC_{LIM_j}\right) = 1 - (1 - 0.001074)(1 - 0.0783) = \mathbf{0.0793}$$

Since when these pulses are present, they completely saturate the receiver, the other aggregate RFI parameter, R_I, is essentially zero.

4.1.3 Pulse width correction in the pulsed duty cycle parameter formula for EESS chirp effect

The pulse width (PW_i) component of the single source saturating pulsed duty cycle, $PDC_{LIM,i}$ formula, equation (13), needs to be modified if the pulse source bandwidth does not fall completely within the RNSS receiver passband. An example case is an EESS (active) spaceborne radar (1 215-1 300 MHz) with relatively wide intra-pulse frequency chirp. To correct for the portion of a frequency chirp that falls outside the RNSS receiver passband, the transmit PW_i component is replaced by: $PW_{i,eff} = PW_{i*} (BW_{overlap}/BW_{chirp})$, where $BW_{overlap}$ is the amount of the total transmit chirp width that falls within the receiver pre-correlator bandwidth.

4.1.4 PRF correction in the pulsed duty cycle parameter formula for EESS scanning effects on semi-codeless RNSS receivers

Testing of an EESS rapid-scanning beam against some semi-codeless RNSS receivers that use very narrow tracking loop bandwidths has indicated that the PRF_i component of the single source saturating pulsed duty cycle, $PDC_{LIM,i}$ formula, equation (13), may be modified. In particular, this testing showed that to correct for the fast azimuth beam scanning of scatterometer type EESS active spaceborne sensors, the PRFi term in equation (13) is replaced by $PRF_{i,efff} = PRF_i * \tau_{obs}/Tc$ where τ_{obs} is the portion of the overall beam scanning period, *Tc*, in which the received power is above the RNSS receiver input compression point. It is important to note that application of this correction factor is only valid when the receiver employs a very narrow (e.g. 0.05 Hz) tracking loop bandwidth. Further studies contained in Report ITU-R M.2496 provide the technical rationale that this correction is not appropriate for all RNSS receivers, and it should not be assumed in general analyses.

4.2 High-precision receiver aggregate pulsed RFI parameters

4.2.1 High-precision CDMA receiver pulsed RFI parameters

The high-precision CDMA receiver operates in the 1 164-1 215 MHz band with an RNSS signal carrier frequency at 1 176.45 MHz. As a dual- or triple-frequency receiver, it also operates simultaneously in the bands 1 215-1 300 MHz and 1 559-1 610 MHz (RNSS signal carrier frequencies at 1 227.6 and 1 575.42 MHz, respectively). The receiver is assumed to saturate on strong pulses. Other pertinent characteristics are listed in Table 10.

TABLE 10

High-precision CDMA receiver pulse response characteristics[17]

Characteristic	Value
Maximum receive antenna gain – lower hemisphere (dBi)	−7.0 (1)
RF filter 3 dB bandwidth (MHz)	24
Receiver input saturation level (dBW)	−120
Receiver survival level (dBW)	−20
Receiver overload recovery time (s)	1×10^{-6}

(1) This value applies for elevation angles ≤ +10° with respect to the horizon.

The pulsed RF sources for this example are assumed to be three ARNS ground beacon (TACAN) stations[18] operating in the 1 100-1 213 MHz band and located on the ground a few kilometres from the high-precision CDMA receiver. A representative limiting-case scenario location is illustrated in Fig. 14 above; where the RNSS receiver is midway between TACAN stations #2, #3, and #5 south of Baltimore, MD, USA. The radial separation is such that the received peak RFI pulse level is above the receiver saturation level but below the survival level. The centre frequencies for the three ARNS transmitters lie within the receiver RF 3 dB bandwidth (i.e. 1 164.5 to 1 188.45 MHz). Other pertinent characteristics are listed in Table 11. Annex A, Table 15 lists additional station parameters.

TABLE 11

ARNS beacon transmission characteristics

Characteristic	Value
Transmitter peak power (dBW)	35.44
Antenna gain (0° elev.) (dBi)	0
Transmit pulse width (s) (per pulse)	3.5×10^{-6}
Transmit pulse pair repetition rate (s^{-1})	3 600

Since there are three saturating pulse sources in this example, the aggregate RFI total pulse duty cycle parameter, PDC_{LIM}, from § 2.3.2 of this Report is computed with a form of equation (5) from § 2.3.1:

---

17 These RNSS receiver characteristic values are taken from Recommendation ITU-R M.1905 for the 1 164-1 215 MHz band, Annex 2, Table 1, Column 3 (except for pulse response parameters which are chosen by similarity with the receiver in § 4.2.2 below). See also Footnote 20.

18 See DME/TACAN beacon description in § 3.1.1 above.

$$PDC_{LIM} = 1 - \prod_j (1 - PDC_{LIMj})$$

where the symbol $\prod_j$ denotes multiplication carried over the individual source index, j (= 1, 2, 3).

The individual TACAN beacon limiting duty cycle, PDC_{LIMj}, is determined using (13) as follows:

$$PDC_{LIMj} = 2 \cdot (PW + \tau_R) \cdot PRF$$

where:

PW: TACAN individual pulse width (3.5 μs)

τ_R: RNSS receiver overload recovery (1 μs)

PRF: pulse pair repetition rate (3600 pulses/s).

Therefore in this example each single TACAN source $PDC_{LIMj} = 2 \cdot (3.5 + 1) \cdot 3600 \cdot 10^{-6} = 0.0324$ and thus the aggregate $PDC_{LIM} = 1 - (1 - .0324)^3 = 0.09408$.

Since when these pulses are present, they completely saturate the receiver, the other aggregate RFI parameter, R_I, is essentially zero.

4.2.2 GPS high-precision semi-codeless receiver pulsed RFI parameters

The high-precision semi-codeless receiver operates as a dual-frequency receiver in the 1 215-1 300 MHz band with an RNSS signal carrier frequency signal at 1 227.6 MHz and simultaneously in the 1 559-1 610 MHz band (RNSS signal carrier frequency at 1 575.42 MHz). The receiver is assumed to saturate on strong pulses. Other pertinent characteristics are listed in Table 12.

The pulsed RF source for this example is assumed to be a single surveillance radar transmitter system operating in the 1 215-1 390 MHz band[19] and located on the ground a few kilometres from the RNSS receiver. The separation is such that the received peak RFI pulse level is above the receiver saturation level but below the survival level. The centre frequency for the radar pulses is assumed to lie within the receiver RF 3 dB bandwidth (i.e. 1 215.6 to 1 239.6 MHz). Other pertinent characteristics are listed in Table 9.

TABLE 12

High-precision semi-codeless receiver pulse response characteristics[20]

Characteristic	Value
Maximum receive antenna gain – lower hemisphere (dBi)	−7.0 (1)
RF filter 3 dB bandwidth (MHz)	24
Receiver input saturation level (dBW)	−120
Receiver survival level (dBW)	−20
Receiver overload recovery time (s)	1×10^{-6}

(1) This value applies for elevation angles ≤ +10° with respect to the horizon.

19 See description in § 4.1 above.

20 These RNSS receiver characteristic values are taken from Recommendation ITU-R M.1905 for the 1 164-1 215 MHz band, Annex 2, Table 1, Column 3 (except for pulse response parameters chosen by similarity to Column 1).

The radar beam scanning is such that the high-precision semi-codeless receiver is mostly illuminated by the radar beam side lobes (at 40 dB below the main beam). At a nominal spacing (several tens of km) from the SBAS receiver, free-space propagation calculations show the sidelobe received peak level is 64.8 dB above the receiver saturation level and the main beam peak level is 20.2 dB below the receiver survival level.

Since there is only a single (saturating) pulse source in this example, the aggregate RFI total pulse duty cycle parameter, PDC_{LIM}, from § 2.3.2 of this Report is computed simply as follows:

$$PDC_{LIM} = (PW + \tau_R) \cdot PRF$$

where:

PW : radar pulse width (50 μs)

τ_R : receiver overload recovery (1 μs)

PRF : radar pulse repetition rate (1 500 pulses/s).

Therefore in this example, $PDC_{LIM} = (50 + 1) \cdot 1500 \cdot 10^{-6} = 0.0765$.

Since when these pulses are present, they completely saturate the receiver, the other aggregate RFI parameter, R_I, is essentially zero.

4.3 Pulsed RFI parameter computation examples for High-accuracy and authentication receiver using E6-BC/L6

The RNSS receiver type “High-accuracy and authentication receiver using E6-BC/L6” operates in the 1 215-1 300 MHz band with an RNSS signal carrier frequency signal at 1 278.75 MHz. The RNSS receivers in this category are assumed to include both those employing AGC and those without AGC. As described in § 2.2.4.1, the variation of AGC recovery time should be taken into account in case of the RNSS receiver with AGC. But it should be noted that the AGC recovery time is usually very short, ideally less than 1 μs. The RNSS receiver characteristics relevant to these pulsed interference analyses are listed in Table 13.

TABLE 13

RNSS receiver pulse response characteristics[21]

Characteristic	Value
Maximum receive antenna gain – upper hemisphere (dBi)	3.0
RF filter 3 dB bandwidth (MHz)	40.92 or 42.0
Receiver input saturation level (dBW)	−120
Receiver survival level (dBW)	−20
Receiver overload recovery time (s)	1.0×10^{-6}

The pulsed RF source for this example is assumed to be a single SAR operating in the 1 215-1 300 MHz band. The interference power levels from SAR are such that the received peak RFI pulse level exceeds the RNSS receiver saturation level but is below the survival level. The SAR characteristics used in the analyses are listed in Table 14.

[21] These RNSS receiver characteristic values are taken from Recommendation ITU-R M.1902 for the 1 215-1 300 MHz band, Annex 1, Table 1, Column 3b.

TABLE 14

SAR characteristics[22]

Characteristic	Value
Main beam e.i.r.p. (dBW)	74.5
Orbital altitude (km)	628
RF centre frequency (MHz)	1 257.5
RF bandwidth (MHz)	28
Pulse modulation	Linear FM
Transmit pulse width (s)	(11-49) × 10^{-6}
Pulse repetition frequency, max (s^{-1})	6 000 (1)

(1) In case of transmit pulse width of 11 ms.

Since there is only a single (saturating) pulsed interference source in this example, the aggregate RFI total pulse duty cycle parameter, PDC_{LIM}, from § 2.3.2 of this Report is computed simply as follows:

$$PDC_{LIM} = (PW + \tau_R) \cdot PRF$$

where:

PW : radar pulse width (11 μs)

τ_R : receiver overload recovery time (1 μs), which includes the worst-case AGC recovery for the RNSS receiver with pulse blanking

PRF : radar pulse repetition rate (6 000 pulses/s).

Therefore, in this example, $PDC_{LIM} = (11 + 1) \cdot 6000 \cdot 10^{-6} = 0.072$.

5 Conclusions

This Report describes a method to calculate the aggregate RFI parameters of in-band and near-band pulsed RFI sources that may impact RNSS airborne and ground-based receivers. Detailed applications of the method are given for high- and low-altitude airborne RNSS receivers (1 164-1 188 MHz) and for ground-based receivers (1 164-1 215 and 1 215-1 300 MHz). Aggregate pulsed RFI parameters calculated by the method can be used in the general pulsed RFI impact evaluation method for RNSS receivers that is described in Recommendation ITU-R M.2030. Possible application of the method in this Report to higher frequency RNSS bands could be the subject of further study within the ITU-R.

22 Values are taken from a revision in development within the ITU-R for Recommendation ITU-R RS.1347, Annex, Table 1-1, SAR6.

Annex A

Propagation modelling with the GPS RFI Environmental Evaluation Tool (GREET)

The main use of GREET is to calculate TACAN/DME beacon emitter environment RFI parameters described in § 2.3. GREET first calculates the received power of all TACAN and DME beacon pulses received at the RNSS receiver at various locations (latitude/longitude/altitude) within the region of interest. The above-blanker pulse widths from each of the resulting N_T TACAN and N_D DME emitters within the radio-LoS are then calculated from equation (10) and the above-blanker pulse width expected (average) value $\hat{w}$ is determined (see Annex B). This result is then inserted into the equation for actual blanking duty cycle $PDC_{B,\ DME/TACAN}$ (equation (19)). GREET also computes the residual below-blanker pulse width for strong pulses (equation (11)) which is included with the average power from weak pulses to make up the $R_{I,\ DME/TACAN}$ parameter. Additional details of the GREET tools are described below.

A.1 GREET tool overview

MITRE's Center for Advanced Aviation Systems Development (CAASD) developed GREET to determine the compatibility of the planned GPS L5 signal at 1 176.45 ± 20 MHz with existing systems in 1999. Under the auspices of US Government ad hoc working groups commissioned to determine and validate the compatibility with existing systems, the tool has been periodically updated as ad hoc Working Group 1 (WG 1) and RTCA SC-159 refined the assumptions and methodology for the analyses. The major components of GREET include the following:

– A set of fixed-emitter databases that include radar and DME/TACAN systems from the United States of America and other parts of the world.

– Mobile emitter definition tables that include the parameterized effects of CNI system network and ATCRBS emitters on 1 030 and 1 090 MHz.

– An RFI estimator that determines the aggregate RFI impact by fixed and mobile emitters on an airborne GPS L5 receiver. This is composed of the effective net pulse blanking duty factor (PDCB) and aggregate weak pulse RFI contribution below pulse blanking threshold, R_I, as described in § 2.3.

– A map generator that displays the amount of post-correlation effective S/N degradation expected across each scenario and region studied.

– A Regional RFI database to generate an emulated interfering waveform ensemble assembled from the waveform library composed of DME/TACAN, ATCRBS, TCAS, CNI system, UAT, and radars.

The structure of GREET following the sequence of the modelling functionality, is shown in Fig. 15. The following sections describe the major components of GREET.

FIGURE 15

GREET flow diagram

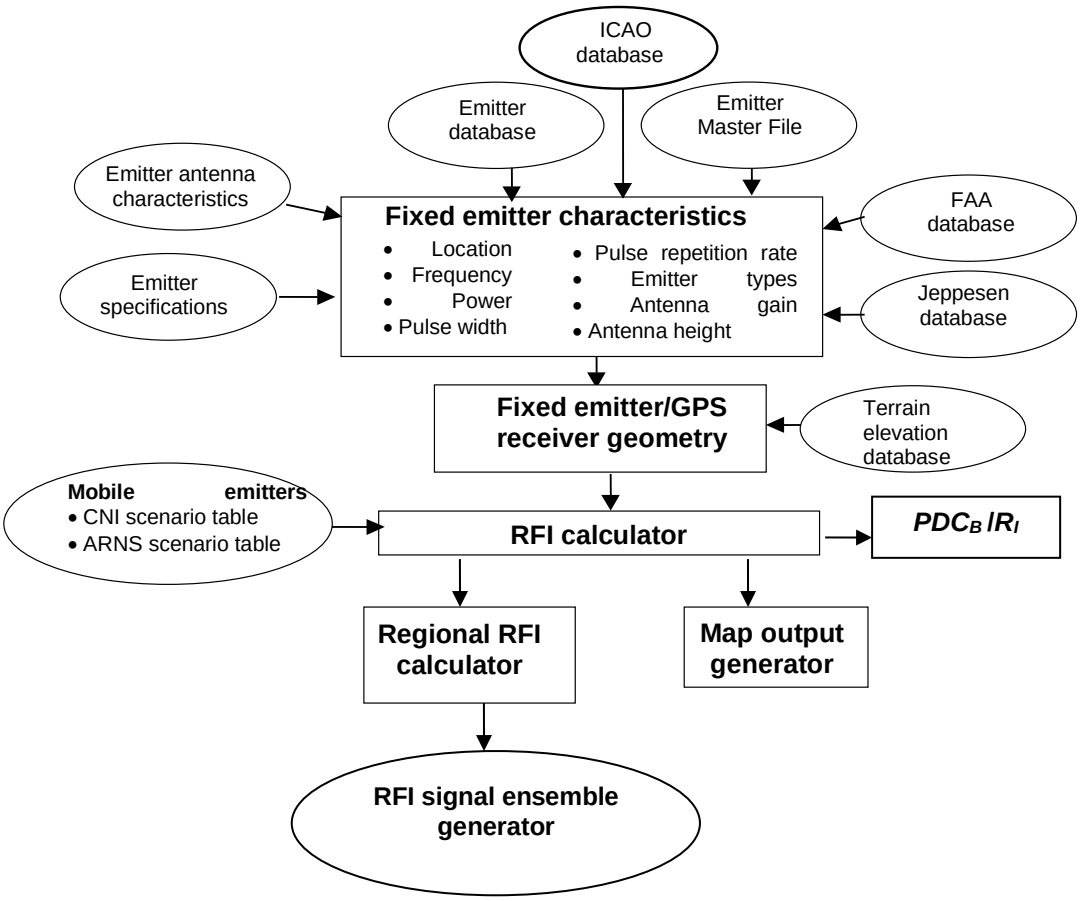

A.2 Fixed emitter database interface

Two fixed emitter databases, one for radar and DME/TACAN, are gathered and updated from various sources.

Radar: The OoB pulsed interference from radars are also considered. The radar carriers are allocated in the 1 215-1 390 MHz band.

For DME/TACAN, the US study uses a combination of the current navaid infrastructure as defined in the FAA Spectrum Engineering Services DME/TACAN database, including Canada and Mexico, and the Jeppesen database for CONUS, Alaska and Hawaii. To determine a power level for each emitter, the FAA ASR authorized power is compared with that assumed from the Jeppesen figure of merit and the maximum of the two is used. For European analysis, ICAO database is used. For studies in other parts of the world, only the Jeppesen database is used, considering figures of merit to determine power levels of the emitters.

A.3 Fixed emitter RFI calculator

This component calculates the aggregate RFI impact that an airborne GPS L5 receiver would experience from the ground-based fixed radar and DME/TACAN sites listed in the databases. For flight altitudes below 18 000 feet, the NIMA digital terrain elevation database is used to accurately represent above ground level (AGL) flight altitudes. For cases above 18 000 feet, altitude above MSL is used without adding ground elevation data. Every half-degree by half-degree latitude and longitude grid point at a given GPS receiver altitude is sampled for radio LoS fixed emitters, and then the aggregate RFI impact, measured in terms of GPS receiver post-correlation SNR reduction, is calculated.

The transmitter and receiver geometry-dependent aggregate RFI calculation is performed as follows:

Bandpass filter preprocessing: Prior to the dynamic link budget computation step, the normalized interference power calculation, independent of geometry, is preprocessed for each emitter that radiates energy through the GPS L5 bandpass filter. This is done by multiplying the GPS receiver bandpass filter squared response by the emitter PSD and integrating the power in the resultant PSD. When this level is adjusted by the transmitter output power, the result corresponds to P_T shown in equation (14) below.

Geometrical link budget calculation: For each 3-D GPS receiver sample point, the set of RLOS ground emitters is identified and their antenna elevation angles and free-space path loss, P_{LOSS}, are calculated. The elevation angles are used to calculate both transmitter and receiver antenna gains. For radar cases, –10 dBi antenna sidelobe gain is uniformly assumed, based on the fact that the exposure to the main beam is rare and strong main beam gain, if any, can be mitigated by GPS L5 pulse blanker circuitry. Normalized DME/TACAN transponder omni azimuth antenna gain patterns, yielding a maximum gain of +6 dBi after the cable loss, are sampled and interpolated as shown in Fig. 5.

The transmitter antenna gain, G_T, and receiver antenna gain, G_R, are used in the received power calculation shown in equation (14), then scaled by the pre-processed bandpass filter response value obtained in the first step above. The result, P_{REC}, corresponds to the undesirable interference power that passes the GPS L5 bandpass filter and enters the pulse blanker.

$$P_{REC}(dB) = P_T(dB) + G_T(dBi) + G_R(dBi) + P_{LOSS}(dB), \tag{14}$$

where:

$$P_{LOSS}(dB) = 20\log_{10}(\lambda/4\pi d) \tag{15}$$

is the free-space path loss defined by the wavelength λ and distance d (m).

The received power from each emitter at each GPS L5 receiver sampling grid point is compared to the GPS L5 receiver blanker threshold for pulse blanker activation. The effective pulse widths of each emitter that causes a received power above this threshold is accumulated into the average above-blanker pulse width, then the net pulse blanking duty cycle PDC_B is computed (equation (19)). For those emitters that cause received powers below the blanker threshold, each power level P_i and duty cycle dc_i is converted to a contribution to the below-blanker interference-to-noise ratio equation (3), then accumulated into total signal to noise ratio reduction, equation (4).

The RFI calculator determines the equation parameters (i.e. PDC_B, R_I) for the fixed emitters and then combines the result with those of ARNS systems and the CNI system to generate aggregate SNR reduction. In each case, the grid points throughout each region assume a uniform amount of RFI contributed by ARNS systems and the CNI system since these are primarily mobile emitters.

A.4 Emulation of DME/TACAN ensemble environment

GREET's ensemble RFI synthesis algorithm can be expressed as:

$$X(t) = \sum_{n=1}^{N_D} \sqrt{P_n} D_n(t + \Delta t_n) \exp\{j(2\pi\Delta f_n + \theta_n)\} + \sum_{n=1}^{N_T} \sqrt{P_n} T_n(t + \Delta t_n) \exp\{j(2\pi\Delta f_n + \theta_n)\} \tag{16}$$

Here, N_D and N_T are the number of DMEs and TACANs included in the emulation, and $D_n(t)$ and $T_n(t)$ represent the waveform templates for DME and TACAN, respectively. The received power, random timing jitter, residual frequency offset between each DME/TACAN carrier and the GPS L5 carrier, and the uniformly distributed random pulse arrival phase (between 0 and 2π) are represented

by $P_n, \Delta t_n, \Delta f_n,$ and $\theta_n,$ respectively. The basic DME template $D_n(t)$ was obtained from the complex waveform as shown in Fig. 16. The basic TACAN template $T_n(t)$ was created in the same manner using a pulse pair repetition period of 1/3 600 ≈ 0.27778 ms.

FIGURE 16

Normalized DME/TACAN complex envelope (Otis AFB, MA TACAN)

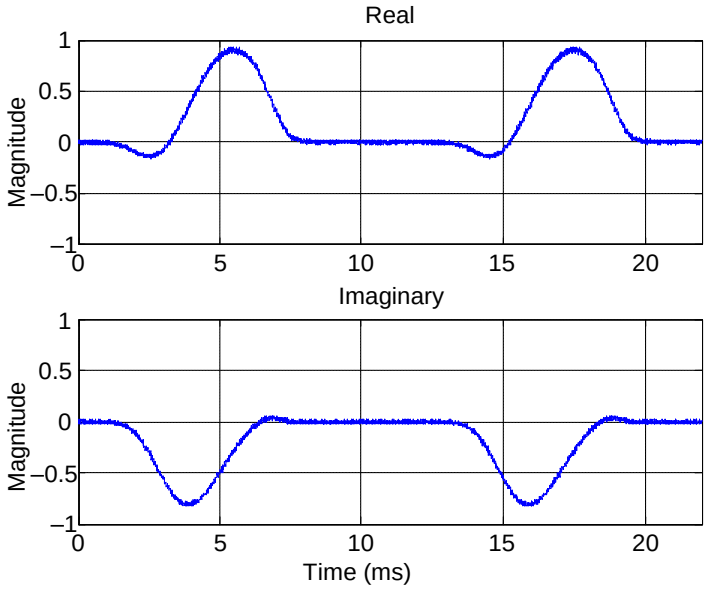

The synthesis algorithm first randomly determines (using a uniform distribution) an initial pulse pair location for the *n*-th emitter's (DME or TACAN) pulse pair within the pulse pair repetition period. This yields a random position of the pulse pair within the template above; then the next occurrence of a pulse pair by the *n*-th emitter is jittered by 10 percent of the repetition cycle. Interrogating pulses are jittered to distinguish themselves from others by time averaging. This amount of jitter is reasonable to account for the randomly inserted dummy transponder reply pulses when the number of interrogations is insufficient to demand a 2 700 ppps response.

A uniformly distributed random phase perturbation is added to each pulse pair occurrence. This process is repeated for each visible DME and TACAN emitter, and the results are summed in a complex manner.

Figure 17 plots an example of the emulated DME/TACAN signals, generated by GREET, that would be seen by a GPS/WAAS L5 receiver at 40 000 feet (ft) above Harrisburg, Pennsylvania. The assumed noise floor in the receiver passband (20 MHz) is at –97 dB(mW).

FIGURE 17

Emulated DME/TACAN environment: 40 kft above Harrisburg, PA

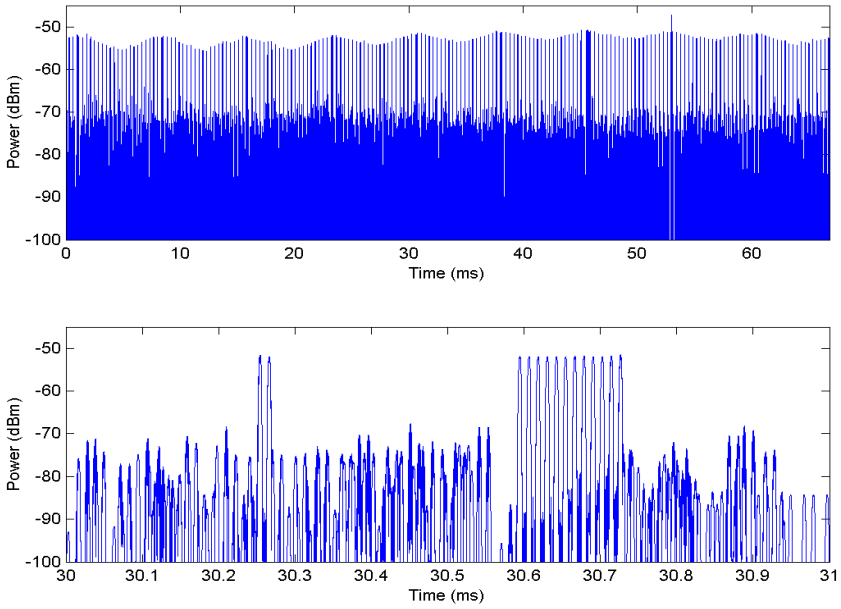

For any given location within the United States of America, GREET calculates a set of output parameters regarding the emissions from visible DME/TACAN beacons. Sample GREET outputs are shown in Table 15 for the DME/TACAN sites near predominantly Harrisburg, Pennsylvania where the GPS L5 receiver was positioned at 76.5 W, 40.5 N, and 40 000 ft above MSL. The output parameters include the transmitter frequency, received power level in dBm, service code for the navaid (1 for DME and 2 for TACAN), and location of each DME/TACAN. Figure 11 shows a map of the GREET results showing the GPS L5 receiver post-correlation effective *S*/*N* degradation due to the aggregate DME/TACANs. Figure 12 shows the additional impact from the CNI system and 1 030/1 090 MHz ARNS systems where the three 'hotspots' are clearly visible.

TABLE 15

GREET-generated GPS L5-interfering DME/TACANs (40 000 ft MSL)

Longitude	Latitude	Alt. (ft)	ERP (dBm)	Freq. (MHz)	Type*	Range (km)	P_{REC} (dBm)	Elev. (deg)	Az. (deg)
−74.96722	39.5375	137	71.4	1 186	2	103.1	−69.8815	6.3	121
−76.59944	40.55333	1 785	71.4	1 180	2	80.8	−70.1192	7.9	50.1
−74.43167	39.81722	246	73	1 168	2	136.3	−70.1582	4.5	99.1
−76.66139	39.17111	167	71.4	1 185	2	108.9	−70.3049	5.9	31.5
−74.49528	40.20222	40	70.8	1 172	2	130.9	−72.1506	4.8	171
−74.80056	39.09528	43	71.4	1 182	2	144.6	−72.1791	4.2	135
−75.60722	39.67806	105	71.4	1 174	2	50.6	−72.2852	13.7	137
−76.74472	38.70583	230	71.4	1 171	2	158	−72.8829	3.7	23.8
−77.95083	39.93306	2 375	71.4	1 184	2	167.4	−73.7627	3.2	86.8
−77.46667	38.93444	335	71.4	1 169	2	173.6	−74.0823	3.2	46.4

TABLE 15 (*end*)

Longitude	Latitude	Alt. (ft)	ERP (dBm)	Freq. (MHz)	Type*	Range (km)	P_{REC} (dBm)	Elev. (deg)	Az. (deg)
−75.67083	39.91806	485	71.4	1 166	2	31.9	−74.647	22	108
−77.97	41.51278	2 356	73	1 173	2	236.9	−76.0014	1.7	44.6
−78.33139	40.735	2 647	71.4	1 183	2	214.7	−76.743	2.1	21.6
−77.35278	38.33639	137	71.4	1 179	2	219.1	−76.9362	2.2	31.9
−74.82194	40.79833	1 063	66	1 176	1	134.3	−77.1283	4.5	139
−78.20556	38.85417	2 457	71.4	1 177	2	229.1	−77.2745	1.8	55.5
−76.775	41.33861	564	66	1 178	1	163	−78.6161	3.5	66
−77.32028	37.50222	196	73	1 175	2	300.6	−79.5321	1	22.1
−76.86611	38.80722	275	71.4	1 165	2	152.6	−80.5581	3.9	29.1
−77.82833	37.52861	475	71.4	1 167	2	317.5	−81.5288	0.7	29.5
−72.31667	40.91889	66	71.4	1 170	2	329.1	−81.8266	0.6	163
−72.94917	42.29111	1 617	71.4	1 185	2	361.5	−83.7632	0.2	136
−80.09917	38.91444	2 175	71.4	1 176	2	373.3	−84.0242	0.1	69.8
−73.60056	41.76972	1 266	66	1 177	1	282.5	−84.193	1.1	137
−73.80306	42.74722	292	71.4	1 187	2	356.7	−86.6637	0.3	122
−79.12111	42.18861	1 814	66	1 181	1	358	−86.8324	0.3	41.8
−74.16	40.31167	167	66	1 188	1	161.1	−87.0301	3.6	168
−73.89472	40.77639	26	66	1 165	1	199	−88.4033	2.6	155
−72.5475	41.64083	866	66	1 183	2	344	−88.8023	0.4	149
−78.83417	40.31667	2 296	73	1 164	2	244.5	−89.7119	1.6	7.4
−77.99278	40.91639	2 457	71.4	1 189	2	197.8	−90.0812	2.4	30.4
−79.10694	37.90028	3 481	66	1 187	1	356.6	−90.5068	0.2	48.2
−75.30306	39.63583	177	71.4	1 162	2	73.2	−94.7363	9.2	124
−74.74194	40.58278	214	66	1 163	1	125.7	−95.6552	5	149
−72.71611	42.16194	305	71.4	1 164	2	366.2	−97.3311	0.2	140
−76.87167	36.37306	413	71.4	1 180	2	410.3	−98.8321	−0.2	10.5
−74.53833	41.0675	1 427	71.4	1 191	2	172	−98.996	3.1	137
−80.74806	41.76	935	71.4	1 186	2	445.8	−99.5536	−0.5	24.5
−78.15306	38.01361	397	71.4	1 190	2	289.3	−100.268	1.1	39.5

NOTE – Type 1 = DME, Type 2 = TACAN.

Annex B

Strong pulse collision model – net PDC_B approach

Section 2.3 uses a model to account for the pulse overlap probability in which the net strong pulse blanking duty cycle from heterogeneous systems operating within the same geographic region is the union of the individual system effects (equation (5)). This model applies equally well for the homogeneous DME/TACAN beacon system RFI analysis since, in regions of high beacon density, the aggregate (gross) blanking duty cycle without overlap consideration can exceed 100%. The basic theory behind the model can be found in various texts on probability and/or queuing theory. A brief summary is provided in the paragraphs below. The overlap probability model was validated by an extensive Monte-Carlo simulation[23].

The general model characterizes the aggregate arrival (reception) rate of strong pulses from randomly generated independent sources as a Poisson process (i.e. the inter-arrival interval between pulse-pair receptions from different beacons is exponentially distributed). In particular, the Poisson probability density function (pdf), p_k, defined as the probability that k arrivals will occur within some arbitrary time interval (t_0, $t_0 + t$), is given as:

$$p_k = \frac{(\lambda t)^k e^{-\lambda t}}{k!} \tag{17}$$

where λ is the average (pulse) arrival rate. The average number of arrivals in the time interval is then λt which has a variance, $\sigma^2 = \lambda t$.

A fundamental property of the underlying exponential inter-arrival distribution is that the process is memory-less; that is, the probability of one or more arrivals in this arbitrary interval does not depend on what occurred prior to time t_0 and the result is valid over any chosen time interval. Thus, the probability of finding no arrivals in an interval of duration, t, is $e^{-\lambda t}$ and, conversely, the probability of finding at least one arrival in the interval is $1-e^{-\lambda t}$. The general model also assumes that each (pulse) arrival in the interval has some finite duration taken as a random variable with arbitrary distribution having an expected (average) value $\hat{w}$ (e.g. above-blanker pulse widths per equation (10) averaged over the beacon emitter set).

Given these two random processes, the general model that accounts for pulse overlays is given as:

$$P_r(\geq arrival\ interval\ \hat{w}) = 1 - e^{-\lambda \hat{w}} \tag{18}$$

which is the steady state probability that at least one arrival occurs during an interval equal to the average pulse duration. The most elegant description of this general model can be obtained from a queuing theory approach[24] characterized by exponential (Memory-less or Markovian) customer inter-arrivals, a general service time distribution and an 'infinite' number of servers (i.e. an M/G/∞ queuing system) which satisfies the ergodicity requirement as long as $\lambda\hat{w}$ is finite. In this context the above result is interpreted as the fraction of time that at least one server is busy with a customer.

---

[23] Op. cit., RTCA/DO-292, Appendix E, § E.5.

[24] Kleinrock, L., *Queuing Systems*, New York, NY, John Wiley & Sons, 1975, Vol. 1, p. 101, Vol. 2, p. 19.

To apply this general model to DME/TACAN beacon RFI receptions, the arrival rate is set to $\lambda = 2\,700N_{DME} + 3\,600N_{TACAN}$ (the aggregate arrival rate of the first pulse of pulse pairs received above blanker threshold); where N_{DME} and N_{TACAN} are the total number of DME and TACAN beacons, respectively, within radio LoS. The average duration, $\hat{w}$, (above-blanker pulse width averaged over the total DME and TACAN received pulses), is set at $\hat{w} = E\{2PW_{eq}\}$. With those values substituted into equation (18), the net pulse blanking duty cycle is given as:

$$PDC_{B,DME/TACAN} = 1 - e^{-\lambda \hat{w}} = 1 - e^{-(2700N_{DME} + 3600N_{TACAN})E\{2PW_{eq}\}} \quad (19)$$